Heterocyclic Letters
Vol. 7| No.3|791-818|May-July| 2017
ISSN : (print) 2231–3087 / (online) 2230-9632
CODEN: HLEEAI
http://heteroletters.org

BIOLOGICAL BEHAVIOR OF QUINAZOLIN-4(3*H*)-ONE DERIVATIVE BASED PLATINUM(II) COMPOUNDS

Miral V. Lunagariya, Khyati P. Thakorand Mohan N. Patel*

**Department of Chemistry, Sardar Patel University,*
Vallabh Vidyanagar–388 120, Gujarat, India.
Corresponding author. Tel.: +91 2692 226856
E-mail: jeenen@gmail.com

Abstract
New series of square planar Pt(II) complexes of the type [$Pt(L^n)(Cl_2)$] [where,L^n = 2-(thiophen-2-yl) quinazolin-4(3H)-one (L^1),2-(5-nitrothiophen-2-yl)quinazolin-4(3H)-one (L^2), 2-(3-methylthiophen-2-yl)quinazolin-4(3H)-one (L^3), 2-(benzo[b]thiophen-2-yl)quinazolin-4(3H)-one (L^4) and 2-(pyridin-2-yl)quinazolin-4(3H)-one (L^5)] have been synthesized and characterized by spectroscopic and physicochemical methods like^{13}C NMR, ^{1}H NMR, mass spectroscopy, TGA and FT-IR,micro-elemental analysis (C, H, N and S), molar conductivity, UV-visible spectra and magnetic susceptibility measurements. The synthesized compounds have been screened for their *in vitro* antibacterial assay against two Gram$^{(+ve)}$ and three Gram$^{(-ve)}$bacterial species. Individual binding constant (K_b), thermodynamics parameters and binding mode of compounds toward herring sperm DNA (HS-DNA) have been determined using absorption titration, viscosity measurement and fluorescence quenching analysis, and concluding the partial intercalative mode of binding. Cytotoxicity profile of the complexes on the brine shrimp shows that the compounds exhibit significant cytotoxic activity with LC_{50}values in the range of6.74 to 100 µg/mL, while cytotoxicity assay with LC_{50} values of cisplatin and transplatin are found 3.133 and 14.45 µg/mL, respectively. The synthesized compounds have been testedfor *in vitro*cellular level cytotoxicity against *S. pombe* cells.Furthermore, dockingassay of the compoundshave been carried out with the aim of findingtheoretical binding free energy and are observed in the range of -193.14 to -252.51 kJmol^{-1}.TheDNA cleavage of all complexes has been examinedusing gel electrophoresis technique and result shows that the complexes cleave of the DNA more efficiently compared to their respective metal salt.The Pt(II) complexes have been also evaluated for their anti-tubercular activity against *Mycobacterium tuberculosis* (Mtb) H_{37}Rv strain.

Keywords: Quinazolinone derivatives scaffold; Platinum(II) complexes; Thermal property; Van't Hoff plots; Cytotoxicity.

1. Introduction

In medicinal inorganic chemistry, one of the most important significance is the unexpected discovery of the cytotoxic properties of cisplatin as an anticancer drugs, which is one of the most commonly used chemotherapeutic agents for treatment of cancer.[I]Although platinum metallo-anticancer drugs such as cisplatin, carboplatin, oxaliplatin and nedaplatin are among the most effective agents for the treatment of cancer.Its clinical utility is restricted due to the frequent development of drug resistance.

Quinazolin-4(*3H*)-ones derivatives are important class of molecules with physiological significance, pharmaceutical utility, synthetic drugs and exhibits wide range of biological activities, such as antidiabetic,[II]antituberculosis,[III]anti-inflammatory,[IV] antifungal,[V] anticancer,[VI] antimicrobial,[III]antimalarial activities,[VII] antiallergy[VIII] andalso their inhibitory effects on thymidylate synthase, poly-(ADP-ribose) polymerase (PARP), and thyrosine kinaseanalgesicproperties.[IX]There are several approved drugs with quinazoline structure in the market such as, prazosin hydrochloride, doxazosine mesylate and terazosine hydrochloride.

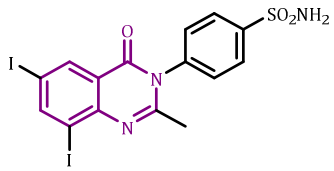

4-(6,8-diiodo-2-methyl-4-oxoquinazolin-3(4*H*)-yl)benzenesulfonamide

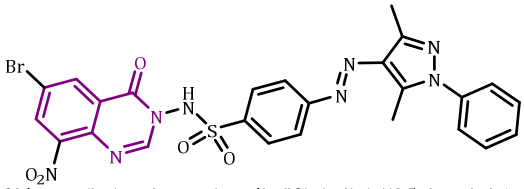

(*E*)-*N*-(6-bromo-8-nitro-4-oxoquinazolin-3(4*H*)-yl)-4-((3,5-dimethyl-1-phenyl-1*H*-pyrazol-4-yl)diazenyl)benzenesulfonamide

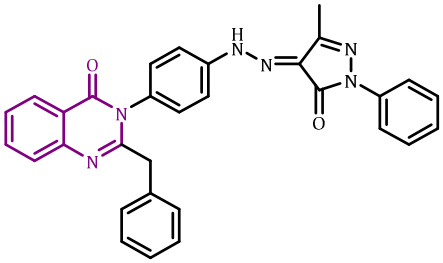

(*E*)-2-benzyl-3-(4-(2-(3-methyl-5-oxo-1-phenyl-1,5-dihydro-4*H*-pyrazol-4-ylidene)hydrazinyl)phenyl)quinazolin-4(3*H*)-one

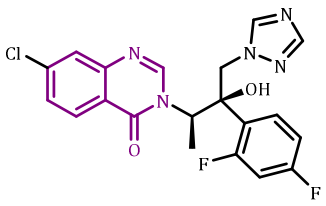

Albaconazole

The substituted quinazolinone derivativesdrugssuch as, 6,8-diiodo-2-methyl-3-substituted-quinazolin-4 (*3H*)-oneswas developed by Raval and co-workers, 4-(3,5-dimethyl-1-phenyl-1H-pyrazol-4-ylazo)-N-(2-substituted-4-oxo-4H-quinazolin-3-yl)benzene sulphonamide derivatives were synthesized by Unnissa and co-workers and also 2- benzyl-3 - {4 - [N '- (3-methyl - 5- oxo - 1,5-dihydropyrazole-4 ylidene) hydrazino phenyl}-3*H*-quinazoline-4-one were developed by Dave and co-workers.[X] The anticancer mechanisms for quinazoline derivatives include inhibition of the DNA repair enzyme system, inhibition ofepidermal growth factor receptor(EGFR), thymidylate enzyme inhibition and inhibitory effects for tubulin polymerize and also enhances the properties of pharmacodynamics, toxicology and efficacy of drugs.[XI,XII]

In the present work,a series of quinazolinone based Pt(II) complexes have been synthesized and characterized by elemental analysis, electronic spectra, conductance measurements, TGA, FT-IR, ^{1}H NMR, ^{13}C NMR, and mass spectroscopy.All synthesized Pt(II) complexes were evaluated for their biological evaluation like*in vitro*antibacterial, cellular level cytotoxicity against *S.pombe* cells, brine shrimp lethality assay, antituberculosis, gel electrophoresis and DNA binding study such as electronic absorption titration with thermodynamics parameters, viscosity measurement, fluorescencequenching analysis

anddocking study. In thecontext of biological significance, we anticipated to develop newapproaches for general structural activity relationship (SAR) diversity of heterocycles incorporatingquinazolinone scaffold.

2. Experimental

2.1 Materials and chemicals

All the chemicals and solvents were of analytical grade and as purchased; MilliQ™ (18.2 m℧, Millipore) was used during the studies.Anthranilamide, benzo[b]thiophene-2-carbaldehyde, 5-nitro thiophene-2-carbaldehyde, 3-methyl thiophene-2-carbaldehyde, thiophene-2-carbaldehyde, pyridine-2-carbaldehyde, $NaHSO_3$, HS DNA and EDTA were purchased from Sigma Aldrich Chemical Co. (India). K_2PtCl_4 salt was purchased from S. D Fine-Chem Ltd. (SDFCL). Agarose, Nutrient broth (NB), ethidium bromide (EtBr), Tris–acetyl–EDTA (TAE), bromophenol blue and xylene cyanol FF were purchased from Himedia (India).*S. pombe*Var. Paul Linder 3360 was obtained from IMTECH, Chandigarh.Thin layer chromatography (TLC) was performed using Merck aluminium sheets coated with silica gel 60 F_{254}. Purification by flash chromatography was performed using Merck silica gel 60. The compounds were visualized under UV light.*S. pombe*Var.Paul Linder 3360 was obtained from IMTECH, Chandigarh.Ethidium bromide. All the bacterial cultures used were purchased from MTCC, Institute of Microbial Technology and Chandigarh, India. An *Artemia cyst was* purchased from local aquarium store. GenElute mini Pre Kit for pUC19 DNA isolation was purchased from Sigma Aldrich (India). HPLC grade DMSO was used to dissolve the platinum compounds.

2.2 Physical measurement

The ^{1}H NMR and ^{13}C NMR were recorded with a Bruker Avance (400 MHz) and (100 MHz). The APT experiment yields methine (CH) and methyl (CH_3) signals negative and quaternary (C) and methylene (CH_2) signals positive. The chemical shift of each resonance was quoted as an estimated midpoint of its multiplicity. The electronic spectra were recorded on a UV-160A UV-vis spectrophotometer, Shimadzu, Kyoto (Japan).IR spectra were recorded on a FT-IR Shimadzu spectrophotometer with sample prepared as KBr pellets in the range 4000–400 cm^{-1}. Elemental analyses (C, H, N and S) were performed with a model *EuroEA* elemental analyser. Fluorescence spectroscopy was carried out by FluoroMax-4, spectrofluorometer, HORIBA (Scientific). Melting points (^{0}C, uncorrected) were determined in open capillaries on hermoCal10 melting point apparatus (Analab Scientific Pvt. Ltd, India). Precoated silica gel plates (silica gel 0.25 mm, 60 G F 254; Merck, Germany) were used for thin layer chromatography. The LC-MS spectra were recorded using Thermo scientific mass spectrophotometer (USA). The magnetic moments were measured by Gouy's method using mercury tetrathiocyanatocobaltate(II) as the calibrant (χ_g=16.44 × 10^{-6} cgs units at 20 °C), citizen balance. Antibacterial study was carried out by means of laminar airflow cabinet Toshiba, Delhi (India). The thermogram of complexes was recorded with a Mettler Toledo TGA/DSC 1 thermogravimetric analyser. Conductance measurement was carried out using conductivity meter model number E-660A. *Photo quantization* of the gel after electrophoresis was done using AlphaDigiDoc™RT. Version V.4.0.0 PC-Image software, California (USA).

2.3 General synthesis of quinazolinone derivativeligands (L^1 –L^5)

To the solution of the anthranilamide (7 mmol), substituted carbaldehydederivatives(7 mmol) were added in the reaction mixture and sodium hydrogen sulphite wasused as a catalystin the presence of solvent dimethylformamide(10 mL), and the resulting reaction mixture was reflux at 150 °C for 6 h,and the progress of the reaction wasmonitored by TLC in every 45 min interval on precoated silica TLC plates by using mixture of solvent like ethyl acetate and hexane use as mobile phase.Upon Completion of the reaction, reaction mixture was allowed

to cooled at room temperature. The mixture was extracted with ethylacetate using brine solution (NaCl) as demulsifier.Extracted organic layer was dried over Na_2SO_4 and evaporated to obtain the precipitate. The obtainedresidue was purified by column chromatography on silica using hexane:ethyl acetate(4:1) system. The obtained fine crystalline product was filtered and dried in a vacuum. The proposed reaction for the synthesis of ligands **(L^1- L^5)** is shown inScheme 1.

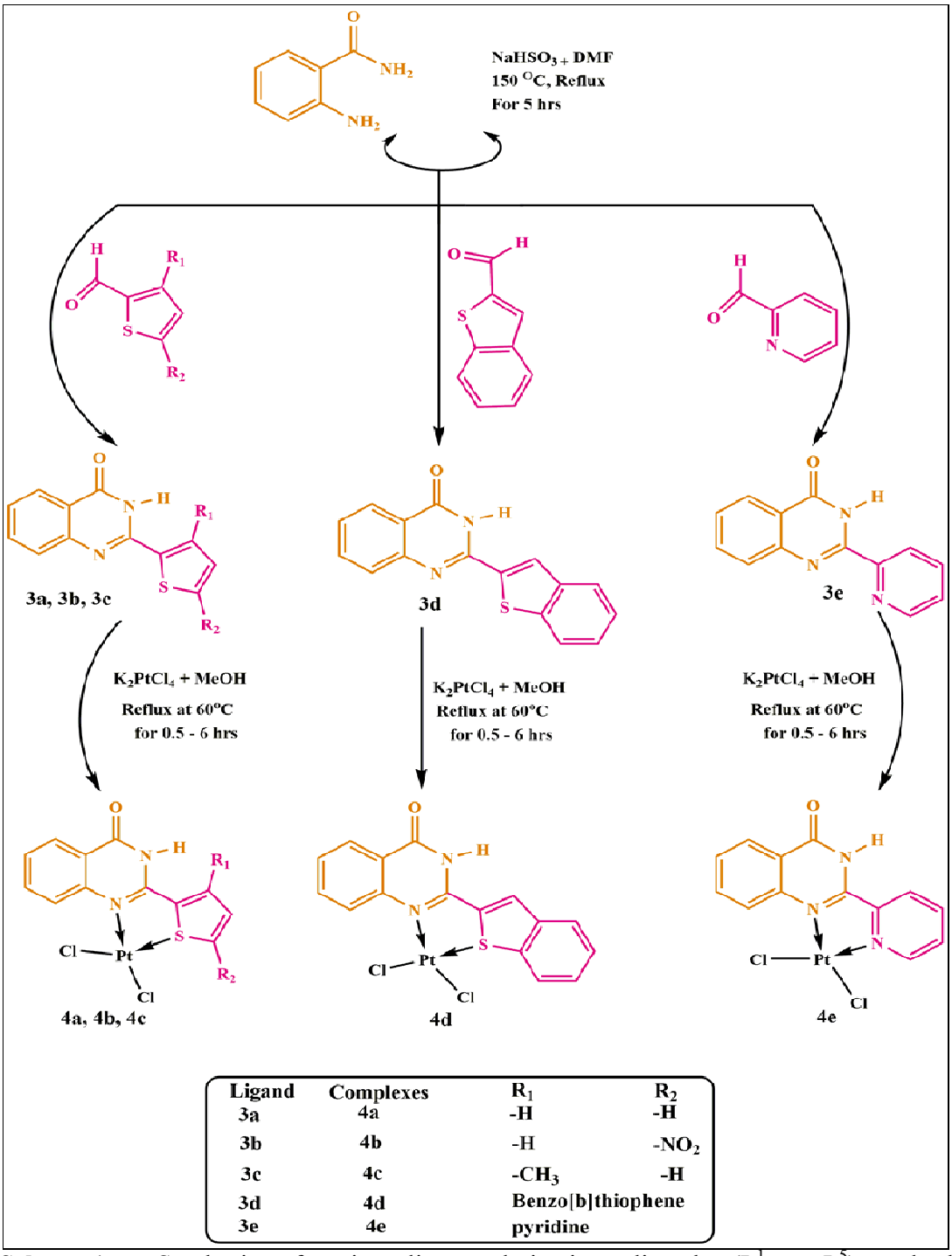

Ligand	Complexes	R_1	R_2
3a	4a	-H	-H
3b	4b	-H	$-NO_2$
3c	4c	$-CH_3$	-H
3d	4d	Benzo[b]thiophene	
3e	4e	pyridine	

Scheme 1. Synthesis of quinazolinone derivatives ligands (L^1 – L^5) and their complexation with Pt^{II} metal ions.

2.3.1 Preparation of 2-(thiophen-2-yl)quinazolin-4(3H)-one (L^1)

It was synthesized using 2-aminobenzamide **(1a)** (0.953 g, 7mmol) and thiophene-2-carbaldehyde (0.784 g, 7mmol) after reflux for 5-6 h in DMF solution as described general process. **Colour**: yellow crystalline solid, **Yield:** 85 %, **mol.wt. :** 228.27g/mol, **m.p.** 240 °C**; Anal. Calc. (%) For $C_{12}H_8N_2OS$:**C, 63.14; H, 3.93; N, 12.87; S, 14.04.**Found (%):** C, 63.38; H, 4.05; N, 13.35; S, 13.2.**UV-vis: λ(nm) (ε, M^{-1} cm^{-1}):** 318 (13,526), 255 (26,666). **Mass m/z (%):** 229 $[M]^+$. **^{1}H NMR (400 MHz, DMSO-d_6) δ/ppm:**9.679(s, 1H, N-H), 7.212-8.334 (7H, m, Ar-$H_{5,6,7,8,3',4',5'}$). **^{13}C NMR (100 MHz, DMSO-d_6) δ/ppm:** 161.00 (>C=O, C_4), 156.23 ($C_{quat.,}$ C_2), 144.51 ($C_{quat.,}$ C_{8a}), 133.42 (CH, C_7), 127.43 (CH, $C_{3'}$), 127.34 (CH, C_6), 127.20 (CH, $C_{4'}$), 126.78 (CH, C_8), 126.65 (CH, C_5), 125.80 (CH, $C_{5'}$), 124.40 ($C_{quat.,}$ $C_{2'}$), 120.80 ($C_{quat,}$ C_{4a}). [**Total signal observed = 12:** signal of C= 5 (quinazolinone-C = 4, thiophene-C = 1), signal of CH = 7 (quinazolinone-CH = 4, thiophene-CH = 3]. **FT-IR: (KBr pellet) ν_{max} (cm^{-1}):**3248 $\nu_{(N-H)}$(s), 1659 $\nu_{(C=O)}$ (s),3086 $\nu_{(=C-H)ar}$ (w), 1419 $\nu_{(C=N)}$ (s), 848 $\nu_{(C-H)banding}$ (s),1589 $\nu_{(C=C)conjugated\ alkenes}$ (s), 910 $\nu_{(C-S-C)stre.\ (thiophene\ ring)}$ (s), 709 – 833 $\nu_{(Ar\ -\ H)2\ adjacent\ hydrogen}$ (s), 586 $\nu_{(=C-H)oop\ band}$ (s).

2.3.2 Preparation of 2-(5-nitrothiophen-2-yl)quinazolin-4(3H)-one (L^2)

It was synthesized using 2-aminobenzamide (0.953 g, 7mmol) and 5-nitrothiophene-2-carbaldehyde (1.106 g, 7mmol) after reflux for 5-6 h in DMF solution as described general process. **Colour:** yellow crystalline solid, **Yield:** 82 %, **mol.wt. :** 273.27 g/mol, **m.p.** 235 °C; **Anal. Calc. (%) For $C_{12}H_7N_3O_3S$:**C, 52.74; H, 2.78; N, 14.18; S, 11.93.**Found (%):** C, 52.98; H, 2.95; N, 13.95; S, 12.02. **UV-vis: λ(nm) (ε, M^{-1} cm^{-1}):** 310 (8,693), 234 (25,926).**Mass m/z(%):** 274 $[M]^+$.**^{1}H NMR (400 MHz, DMSO-d_6) δ/ppm:** 10.130 (s, 1H, N-H), 7.197-7.789 (6H, m,Ar-$H_{5,6,7,8,3',4'}$). **^{13}C NMR (100 MHz, DMSO-d_6) δ/ppm:** 161.00 (>C=O, C_4), 156.23 ($C_{quat.,}$ C_2), 151.21 ($C_{quat.,}$ $C_{5'}$), 144.51 ($C_{quat.,}$ C_{8a}), 133.52 ($C_{quat.,}$ $C_{2'}$), 133.42 (CH, C_7), 128.88 (CH, $C_{4'}$), 128.74 (CH, $C_{3'}$), 127.20 (CH, C_6), 126.78 (CH, C_8), 126.65 (CH, C_5), 120.80 ($C_{quat.,}$ C_{4a}). [**Total signal observed = 12:** signal of C = 6 (quinazolinone-C = 4, thiophene-C = 2), signal of CH = 6 (quinazolinone-CH = 4, thiophene-CH = 2].**FT-IR: (KBr pellet) ν_{max} (cm^{-1}):** 3279 $\nu_{(N-H)}$(s), 1666 $\nu_{(C=O)}$ (s), 3101 $\nu_{(=C-H)ar}$ (w), 1411 $\nu_{(C=N)}$ (s), 864 $\nu_{(C-H)banding}$ (s), 1589 $\nu_{(C=C)conjugated\ alkenes}$ (s), 980 $\nu_{(C-S-C)stre.\ (thiophene\ ring)}$ (s), 709 - 832$\nu_{(Ar\ -\ H)2\ adjacent\ hydrogen}$ (s), 570 $\nu_{(=C-H)oop\ band}$ (s).

2.3.3 Preparation of 2-(3-methylthiophen-2-yl)quinazolin-4(3H)-one (L^3)

It was synthesized using 2-aminobenzamide (0.953 g, 7mmol) and 3-methylthiophene-2-carbaldehyde (0.889 g, 7mmol) after reflux for 5-6 h in DMF solution as described general process. **Colour:** lightyellow crystalline solid, **Yield:** 86 %, **mol.wt. :**242.05 g/mol, **m.p.** 237 °C; **Anal. Calc. (%) For $C_{13}H_{10}N_2OS$:**C, 64.14; H, 4.16; N, 11.88; S, 13.93.**Found (%):** C, 63.90; H, 3.91; N, 12.05; S, 14.10. **UV-vis: λ(nm) (ε, M^{-1} cm^{-1}):**270 (5,020), 250 (21,920).**Mass m/z(%):** 243 $[M]^+$.**^{1}H NMR (400 MHz, DMSO-d_6) δ/ppm:** 10.144 (s, 1H, N-H), 7.226-7.794 (6H, m, Ar-$H_{5,6,7,8,4',5'}$), 0.912 (s, 3H, -CH_3).**^{13}C NMR (100 MHz, DMSO-d_6) δ/ppm:** 161.00 (>C=O, C_4), 156.23 ($C_{quat.,}$ C_2), 144.51 ($C_{quat.,}$ C_{8a}), 139.52 ($C_{quat.,}$ $C_{3'}$), 133.42 (CH, C_7), 130.88 (CH, $C_{4'}$), 130.34 (CH, $C_{5'}$), 127.30 (CH, C_6), 126.78 (CH, C_8), 126.65 (CH, C_5), 120.80 ($C_{quat.,}$ C_{4a}), 120.10 ($C_{quat.,}$ $C_{2'}$), 14.50 (-CH_3). [**Total signal observed = 13:** signal of C = 6 (quinazolinone-C = 4, thiophene-C = 2), signal of CH and CH_3 = 7 (quinazolinone-CH = 4, thiophene-CH = 2, -CH_3 = 1].**FT-IR: (KBr pellet) ν_{max} (cm^{-1}):** 3271 $\nu_{(N-H)}$(s), 1670 $\nu_{(C=O)}$ (s), 3055 $\nu_{(=C-H)ar}$ (w), 1412 $\nu_{(C=N)}$ (s), 833 $\nu_{(C-H)banding}$ (s), 1582 $\nu_{(C=C)conjugated\ alkenes}$ (s), 918 $\nu_{(C-S-C)stre.\ (thiophene\ ring)}$ (s), 710 - 832 $\nu_{(Ar\ -\ H)2\ adjacent\ hydrogen}$ (s), 571 $\nu_{(=C-H)oop\ band}$ (s).

2.3.4 Preparation of 2-(benzo[b]thiophen-2-yl)quinazolin-4(3H)-one (L^4)

It was synthesized using 2-aminobenzamide (0.953 g, 7 mmol) and benzo[b]thiophene-2-carbaldehyde (1.135 g, 7 mmol) after reflux for 5-6 h in DMF solution as described general process. **Colour:** light yellow crystalline solid, **Yield:** 79 %, **mol.wt. :** 278.33 g/mol, **m.p.:** 251 °C; **Anal. Calc. (%) For $C_{16}H_{10}N_2OS$:** C, 69.05; H, 3.62; N, 10.97; S, 12.79. **Found (%):** C, 68.90; H, 3.85; N, 11.35; S, 13.00. **UV-vis: λ(nm) (ε, $M^{-1}cm^{-1}$):** 292 (14,746), 243 (26,666). **Mass m/z(%):** 279 [M]+. **^{1}H NMR (400 MHz, DMSO-d_6) δ/ppm:** 10.148 (s, 1H, N-H), 7.220-7.792 (9H, m, Ar-H5,6,7,8, 3',4',5',6',7'). **^{13}C NMR (100 MHz, DMSO-d_6) δ/ppm:** 161.00 (>C=O, C_4), 156.23 ($C_{quat.}$, C_2), 144.51 ($C_{quat.}$, C_8), 137.82 ($C_{quat.}$, $C_{3'a}$), 135.66 ($C_{quat.}$, $C_{7'a}$), 133.42 (CH, C_7), 127.70 ($C_{quat.}$, $C_{2'}$), 127.30 (CH, C_6), 126.78 (CH, C_8), 126.65 (CH, C_5), 124.40 (CH, $C_{6'}$), 124.30 (CH, $C_{5'}$), 123.80 (CH, $C_{4'}$), 122.20 (CH, $C_{7'}$), 120.80 ($C_{quat.}$, C_{4a}), 110.50 (CH, $C_{3'}$). [**Total signal observed = 16:** signal of C = 7 (quinazolinone-C = 4, bezo[b]thiophene-C = 3), signal of CH = 9 (quinazolinone-CH = 4, bezo[b] thiophene-CH = 5]. **FT-IR: (KBr pellet) ν_{max} (cm^{-1}):** 3279 $\nu_{(N-H)}$ (s), 1651 $\nu_{(C=O)}$ (s), 3055 $\nu_{(=C-H)ar}$ (w), 1434 $\nu_{(C=N)}$ (s), 849 $\nu_{(C-H)banding}$ (s), 1589 $\nu_{(C=C)conjugated\ alkenes}$ (s), 910 $\nu_{(C-S-C)stre.\ (thiophene\ ring)}$ (s), 711 - 835 $\nu_{(Ar - H)2\ adjacent\ hydrogen}$ (s), 570 $\nu_{(=C-H)oop\ band}$ (s).

2.3.5 Preparation of 2-(pyridin-2-yl)quinazolin-4(3H)-one (L^5)

It was synthesized using 2-aminobenzamide (0.953 g, 7mmol) and picolinaldehyde (0.749 g, 7mmol) after reflux for 5-6 h in DMF solution as described general process. **Colour:**brown crystalline solid, **Yield:** 97 %, **mol.wt. :** 223.24 g/mol, **m.p.** 245 °C; **Anal. Calc. (%) For $C_{13}H_9N_3O$:**C, 69.05; H, 4.76; N, 18.32; **Found (%):** C, 68.89; H, 5.09; N, 17.55. **UV-vis: λ(nm) (ε, M^{-1} cm^{-1}):** 307(10,453), 241 (26,266).**Mass m/z (%):** 224 $[M]^+$.**^{1}H NMR (400 MHz, DMSO-d_6) δ/ppm:** 10.123 (s, 1H, N-H), 7.207-7.781 (8H, m, Ar-$H_{5,6,7,8,3',4',5',6'}$).**^{13}C NMR (100 MHz, DMSO-d_6) δ/ppm:** 161.00 (>C=O, C_4), 156.23 ($C_{quat.}$, C_2), 154.21 ($C_{quat.}$, $C_{2'}$), 149.61 (CH, $C_{6'}$), 144.51 ($C_{quat.}$, C_{8a}), 136.12 (CH, $C_{4'}$), 133.42 (CH, C_7), 127.88 (CH, C_8), 127.20 (CH, C_6), 126.78 (C_5, -CH), 125.35 (CH, $C_{5'}$), 120.80 ($C_{quat.}$, C_{4a}), 120.60 (CH, $C_{3'}$). [**Total signal observed = 13:** signal of C = 5 (quinazolinone-C = 4, pyridine-C = 1), signal of CH = 8(quinazolinone-CH = 4, pyridine-CH = 4].**FT-IR: (KBr pellet) ν_{max} (cm^{-1}):** 3248 $\nu_{(N-H)}$(s), 1673 $\nu_{(C=O)}$ (s), 2923 $\nu_{(=C-H)ar}$ (w), 1479 $\nu_{(C=N)}$ (s), 803 $\nu_{(C-H)banding}$ (s),1604 $\nu_{(C=C)conjugated\ alkenes}$ (s), 949 $\nu_{(C-S-C)stre.\ (thiophene\ ring)}$ (s), 713 - 836ν($_{Ar - H)2\ adjacent\ hydrogen}$ (s), 572 $\nu_{(=C-H)oop}$ band (s).

2.4 General synthesis of platinum(II) complexes (I-V)

Herein, we report newfive mononuclear Pt(II) complexes**(I-V)**with the bidentate quinazolinone derivative ligands having -N, S/ -N, N-donor atoms. The complexes were synthesized using method proposed by Hodges and Rund.[XIII]An aqueous solution of K_2PtCl_4salt 2 mL (1 mmol)was mixed with a equimolar amount of theligands(1 mmol)**(L^1 – L^5)** in MeOH (20 mL)at 60 °C with 1-2 drops of hydrochloric acid (free acid is to avoid displacement of Cl^- by -OH) until the solution became colourless (0.5-6 h). Within this period, brown colour precipitates of the platinum(II) complexes were obtained. Reaction mixture was allowed to cool at room temperature and filtered off. The products were collected after washing withmethanol-water (MeOH: H_2O, 1:4) system twice. Which were filtered and dried in a vacuum.[XIV] The reaction scheme for the synthesis of complexes (I-V) is shown in Scheme 1.

2.4.1 Preparation of complex [Pt(L^1)Cl_2] (I)

It was synthesized using potassium tetrachloroplatinate salt (K_2PtCl_4) (0.103 g, 0.25mmol) and ligands (L^1) (0.057 g, 0.25 mmol) 1: 1 ratio, after reflux for 6 h in MeOH/H_2O system as described general process. **Colour:** brown powder, **Yield:** 95 %, **mol.wt.** : 494.26 g/mol, **m.p.**>300 °C; **Anal. Calc. (%) For$C_{12}H_8Cl_2N_2OPtS$:**C, 30.86; H, 1.77; N, 5.67; Pt, 39.97; S, 6.49.**Found (%):**C, 30.76; H, 1.98; N, 5.47; Pt, 40.08; S, 5.79. **Conductance:** 24 Ω$^-$

$^{1}cm^{2}mol^{-1}$.**UV-vis: λ(nm) (ε, M^{-1} cm^{-1}):** 376 (6,053), 323 (13,593), 253 (26,666). **^{1}H NMR (400 MHz, DMSO-d_6) δ/ppm:** 12.08 (s, 1H, N-H), 7.145-8.116 (7H, m, Ar-$H_{5,6,7,8,3',4',5'}$). **^{13}C NMR (100 MHz, DMSO-d_6) δ/ppm:** 161.00 (>C=O, C_4), 159.93 ($C_{quat.,}$ C_2), 142.51 ($C_{quat.,}$ C_{8a}), 139.92 (CH, $C_{3'}$), 139.42 (CH, $C_{4'}$), 134.44 (CH, C_7), 132.92 ($C_{quat.,}$ C_{4a}), 128.20 (CH, C_6), 127.78 (CH, C_5), 125.40 (CH, C_8), 116.90 ($C_{quat.,}$ $C_{2'}$), 116.00 (CH, $C_{5'}$). [**Total signal observed = 12:** signal of C = 5 (quinazolinone-C = 4, thiophene-C = 1), signal of CH = 7(quinazolinone-CH = 4, thiophene-CH = 3]. **FT-IR: (KBr pellet) ν_{max} (cm^{-1}):** 3309$\nu_{(N-H)}$(s), 1643 $\nu_{(C=O)}$ (s), 3070 $\nu_{(=C-H)ar}$ (w), 1473 $\nu_{(C=N)}$ (s), 756 $\nu_{(C-H)banding}$ (s),1566 $\nu_{(C=C)conjugated\ alkenes}$ (s), 1188 $\nu_{(C-S-C)stre.\ (thiophene\ ring)}$ (s), 715 - 836 $\nu_{(Ar - H)2\ adjacent\ hydrogen}$ (s), 570 $\nu_{(=C-H)oop\ band,}$ 686 $\nu_{(Pt-S)}$ (s).

2.4.2 Preparation of complex [Pt(L^2)Cl_2] (II)

It was synthesized using potassium tetrachloroplatinate salt (K_2PtCl_4) (0.103 g, 0.25mmol) and ligands (L^2) (0.068 g, 0.25mmol) 1:1 ratio, after reflux for 6 h in MeOH/H_2O system as described general process. **Colour:** brown powder, **Yield:** 90 %, **mol.wt. :** 539.26 g/mol, **m.p.**>300 °C; **Anal. Calc. (%) For $C_{12}H_7Cl_2N_3O_3PtS$:** C, 26.83; H, 1.91; N, 7.79; Pt, 36.88; S, 5.02.**Found (%):** C, 27.26; H, 2.08; N, 8.17; Pt, 37.30; S, 4.95.**Conductance:** 22 $\Omega^{-1}cm^{2}mol^{-1}$. **UV-vis: λ(nm) (ε, M^{-1} cm^{-1}):** 383 (2,493), 314 (7,460), 252 (24,486). **^{1}H NMR (400 MHz, DMSO-d_6) δ/ppm:** 12.55 (s, 1H, N-H), 7.246-7.837 (6H, m, Ar-$H_{5,6,7,8,3',4'}$). **^{13}C NMR (100 MHz, DMSO-d_6) δ/ppm:** 161.00 (>C=O, C_4), 159.93 ($C_{quat.,}$ C_2), 142.55 ($C_{quat.,}$ C_{8a}), 139.92 (CH, $C_{3'}$), 138.42 (CH, $C_{4'}$), 136.44 ($C_{quat.,}$ $C_{5'}$), 134.54 (CH, C_7), 132.92 ($C_{quat.,}$ C_{4a}), 128.20 (CH, C_6), 127.78 (CH, C_5), 125.40 (CH, C_8), 116.90 (Cquat., $C_{2'}$). [**Total signal observed = 12:** signal of C= 6 (quinazolinone-C = 4, thiophene-C = 2), signal of CH = 6 (quinazolinone-CH = 4, thiophene-CH = 2].**FT-IR: (KBr pellet) ν_{max} (cm^{-1}):** 3340 $\nu_{(N-H)}$(s), 1644 $\nu_{(C=O)}$ (s), 3109 $\nu_{(=C-H)ar}$ (w), 1458 $\nu_{(C=N)}$ (s), 756 $\nu_{(C-H)banding}$ (s),1573 $\nu_{(C=C)conjugated\ alkenes}$ (s), 1141 $\nu_{(C-S-C)stre.\ (thiophene\ ring)}$ (s), 715 - 836 $\nu_{(Ar - H)2\ adjacent\ hydrogen}$ (s), 570 $\nu_{(=C-H)oop\ band,}$ 625 $\nu_{(Pt-S)}$ (s).

2.4.3 Preparation of complex [Pt(L^3)Cl_2] (III)

It was synthesized using potassium tetrachloroplatinate salt (K_2PtCl_4) (0.103 g, 0.25mmol) and ligands (L^3) (0.060 g, 0.25 mmol) 1: 1 ratio, after reflux for 6 h in MeOH/H_2O system as described general process. **Colour:** brown powder, **Yield:** 92 %, **mol.wt. :**506.95 g/mol, **m.p.**>300 °C; **Anal. Calc. (%) For $C_{13}H_{10}Cl_2N_2OPtS$:**C, 30.82; H, 1.98; N, 5.71; Pt, 38.79; S, 6.78.**Found (%):**C, 30.88; H, 2.28; N, 5.32; Pt, 39.18; S, 7.11.**Conductance:** 23 $\Omega^{-1}cm^{2}mol^{-1}$. **UV-vis: λ(nm) (ε, M^{-1} cm^{-1}):** 350.05 (6,446), 318 (10,613), 253 (26,666). **^{1}H NMR (400 MHz, DMSO-d_6) δ/ppm:** 12.97 (s, 1H, N-H), 7.386-7.830 (6H, m, Ar-$H_{5,6,7,8,4',5'}$), 1.243 (s, 3H, -CH_3).**^{13}C NMR (100 MHz, DMSO-d_6) δ/ppm:** 161.00 (>C=O, C_4), 159.93 ($C_{quat.,}$ C_2), 144.45 ($C_{quat.,}$ C3'), 142.55 ($C_{quat.,}$ C_{8a}), 139.92 (CH, $C_{4'}$), 134.54 (CH, C_7), 132.92 ($C_{quat.,}$ C_{4a}), 128.20 (CH, C_6), 127.78 (CH, C_5), 125.40 (CH, C_8), 116.00 (CH, $C_{5'}$), 109.00 ($C_{quat.,}C_{2'}$), 18.00 (CH_3). [**Total signal observed = 13:** signal of C = 6 (quinazolinone-C = 4, thiophene-C =2), signal of CH and CH_3 = 7 (quinazolinone-CH = 4, thiophene-CH = 2, -CH_3- 1].**FT-IR: (KBr pellet) ν_{max} (cm^{-1}):** 3440 $\nu_{(N-H)}$(s), 1674 $\nu_{(C=O)}$ (s), 3078 $\nu_{(=C-H)ar}$ (w), 1466 $\nu_{(C=N)}$ (s), 764 $\nu_{(C-H)banding}$ (s),1566 $\nu_{(C=C)conjugated\ alkenes}$ (s), 1142 $\nu_{(C-S-C)stre.\ (thiophene\ ring)}$ (s), 710 - 835$\nu_{(Ar - H)2\ adjacent\ hydrogen}$ (s), 571 $\nu_{(=C-H)oop\ band,}$ 625 $\nu_{(Pt-S)}$ (s).

2.4.4 Preparation of complex [Pt(L^4)Cl_2] (IV)

It was synthesized using potassium tetrachloroplatinate salt (K_2PtCl_4) (0.103 g, 0.25mmol) and ligands (3d) (0.069 g, 0.25mmol) 1: 1 ratio, after reflux for 6 h in MeOH/H_2O system as described general process. **Colour:** brown powder, **Yield:** 92 %, **mol.wt. :** 544.32 g/mol, **m.p.**>300 °C; **Anal. Calc. (%) For $C_{16}H_{10}Cl_2N_2OPtS$:** C, 35.91; H, 1.85; N, 5.95; Pt, 35.04; S, 5.99.**Found (%):**C, 36.11; H, 2.05; N, 6.15; Pt, 34.84; S, 6.19.**Conductance:** 20 $\Omega^{-1}cm^{2}mol^{-1}$. **UV-Vis: λ(nm) (ε, M^{-1} cm^{-1}):** 330.05 (15,806), 317 (15,886), 258 (23,473).**^{1}H**

NMR (400 MHz, DMSO-d_6) δ/ppm:12.87 (s, 1H, N-H), 7.361-8.177 (9H, m, Ar-$H_{5,6,7,8,3',4',5',6',7'}$).**^{13}C NMR (100 MHz, DMSO-d_6) δ/ppm:** 161.00 (>C=O, C_4), 159.93 ($C_{quat.}$, C_2), 143.95 ($C_{quat.}$, $C_{7'a}$), 142.45 ($C_{quat.}$, C_{8a}), 141.55 (CH, $C_{3'}$), 136.92 ($C_{quat.}$, $C_{3'a}$), 134.54 (CH, C_7), 132.54 ($C_{quat.}$, C_{4a}), 132.22 (CH, $C_{5'}$), 128.78 (CH, C_6), 128.08 (CH, $C_{4'}$), 127.90 (CH, $C_{6'}$), 127.78 (CH, C_5), 125.50 (CH, C_8), 125.10 (CH, $C_{7'}$), 112.00 ($C_{quat.}$, $C_{2'}$). [**Total signal observed = 16:** signal of C = 7 (quinazolinone-C = 4,benzo[b]thiophene-C = 3), signal of CH = 9 (quinazolinone-CH = 4, benzo[b]thiophene-CH = 5].**FT-IR: (KBr pellet) ν_{max} (cm^{-1}):** 3471 $\nu_{(N-H)}$(s), 1674 $\nu_{(C=O)}$ (s), 3078 $\nu_{(=C-H)ar}$ (w), 1466 $\nu_{(C=N)}$ (s), 771 $\nu_{(C-H)banding}$ (s),1566 $\nu_{(C=C)conjugated\ alkenes}$ (s), 1134 $\nu_{(C-S-C)stre.\ (thiophene\ ring)}$ (s), 711 - 835 $\nu_{(Ar-H)2\ adjacent\ hydrogen}$ (s), 570 $\nu_{(=C-H)oop\ band,}$ 632 $\nu_{(Pt-S)}$ (s).

2.4.5 Preparation of complex [Pt(L^5)Cl$_2$] (V)

It was synthesized using potassium tetrachloroplatinate salt (K_2PtCl_4) (0.103 g, 0.25mmol) and ligands (L^5) (0.055 g, 0.25mmol) 1: 1 ratio, after reflux for 6 h in MeOH/H_2O system as described general process. **Colour:** brown powder, **Yield:** 90 %, **mol.wt. :**487.98g/mol, **m.p.** >300 °C; **Anal. Calc. (%) For $C_{13}H_9Cl_2N_3OPt$:** C, 31.94; H, 1.85; N, 8.09; Pt, 39.18.**Found (%):**C, 31.71; H, 1.83; N, 7.75; Pt, 38.84.**Conductance:** 20 $\Omega^{-1}cm^2mol^{-1}$. **UV-vis: λ(nm) (ε, M^{-1} cm^{-1}):** 377.05 (2,553), 306 (10,040), 246 (26,666).**LC-MS m/z (%):**487.98 [M], 489.97 [M + 2], 491.98 [M + 4]. **^{1}H NMR (400 MHz, DMSO-d_6) δ/ppm:** 13.63 (s, 1H, N-H), 7.456-8.172 (8H, m, Ar-$H_{5,6,7,8,3',4',5',6'}$). **^{13}C NMR (100 MHz, DMSO-d_6) δ/ppm:** 161.00 (>C=O, C_4), 155.93 ($C_{quat.}$, C_2), 154.73 ($C_{quat.}$, $C_{2'}$), 146.45 (CH, $C_{4'}$), 144.45 (CH, $C_{6'}$),142.55 ($C_{quat.}$, C_{8a}), 134.54 (CH,C_7), 132.92 ($C_{quat.}$, $C_{4'a}$), 129.20 (CH, $C_{3'}$), 128.90 (CH, C_6), 128.20 (CH, $C_{5'}$), 127.78 (CH, C_5), 125.40 (CH, C_8). **[Total signal observed = 13:** signal of C = 5 (quinazolinone-C = 4, pyridine-C = 1), signal of CH = 8 (quinazolinone-CH = 4, pyridine-CH = 4].**FT-IR: (KBr pellet) ν_{max} (cm^{-1}):** 3363 $\nu_{(N-H)}$(s), 1682 $\nu_{(C=O)}$ (s), 3063 $\nu_{(=C-H)ar}$ (w), 1474 $\nu_{(C=N)}$ (s), 772 $\nu_{(C-H)banding}$ (s), 1543 $\nu_{(C=C)conjugated\ alkenes}$ (s), 1103 $\nu_{(C-S-C)stre.\ (thiophene\ ring)}$ (s), 711 - 835 $\nu_{(Ar-H)2\ adjacent\ hydrogen}$ (s), 570 $\nu(=C-H)_{oop\ band}$, 578 $\nu_{(Pt-N)}$ (s).

2.5 Biological application of Pt(II) complexes

2.5.1 In vitro antimicrobial assay

To studythe antibacterial activity of compounds under investigation, we used five microorganism: two Gram$^{(+ve)}$*(Bacillus subtilis* (MTCC 7193)and*Staphylococcus aureus* (MTCC 3160)) and three Gram$^{(-ve)}$ (*Escherichia coli* (MTCC 433), *Pseudomonas aeruginosa* (MTCC P-09) and*Serratia marcescens* (MTCC 7103)). DMSO was used as medium to acquire preferred concentration of compounds to check upon microbial strains. MIC was performed by broth dilution technique. A prelature of bacteria was used to prepare bacterial cultures in Luria Broth. The test compounds of specific concentration were added to the corning tube containing Luria Broth solution and sterilized before the addition of previously cultured bacterial species. After adding different bacterial species to the tubes containing a specific concentration of test compounds, it was allowed to incubate for 24 h. at optimum temperature. The experiment is repeated till only a faint turbidity appears in the tube. The lowest concentration, which showed no visible growth after 24 h subculture was considered as MIC for each compound.[XIV]

2.5.2 Cellular level bioassay using Schizosaccharomyces Pombe cells

Cellular level bioassay was carried out using*S. pombe*cells, which were grown in liquid yeast extract media in 150 mL Erlenmeyer flask containing 30 mL of yeast extract media. The flask was incubated at 30 ^{0}C on a shaker at 160 rpm till the exponential growth of*S. pombe*obtained (24 to 30 h). Then the cell culture was treated with the differconcentrations (20, 40, 60, 80, 100 μM) of synthesized complexes, free ligands and also with DMSO as a control and further allowed to grow for 20-24 h. Next day, by centrifugation at 12,000 rpm 10

min; treated cells were collected and dissolved in 500mL of PBS (Phosphate Buffered Saline). The 80mL of yeast culture dissolved in PBS and 20mL of 0.4% trypan blue prepared in PBS were mixed and cells were observed in a compound microscope (40 X). The trypan blue dye could enter the dead cell only so they appeared blue, whereas live cells resisted the entry of dye. The number of dead cells and number of live cells was counted in one field. Cell counting was repeated in two more of the microscopic fields and average percentage of cells died due to synthesized compounds were calculated.[XV]

2.5.3 In vitro Mycobacterium tuberculosis study using a strain of $H_{37}Rv$

A primary *in vitro* antituberculosis activity of the synthesized Pt(II) complexes (I-V) were conducted at a concentration of 250 µg/mLagainst *Mycobacterium* tuberculosis $H_{37}Rv$ strain by using Lowenstein - Jensen medium as described by Rattan.[XVI]

2.5.4 In vitro cytotoxicity bioassay

The treatment of cancer is limited to surgery, radiotherapy and the use of cytotoxic agents, regardless of their well-known side effects. However, as no curative therapy is available and the discovery and development of novel, active chemotherapeutic agents is desperately needed. For the development of new drugs, primary study involves the brine shrimp lethality bioassay.Cytotoxicity assays are widely used by the pharmaceutical industry to screen for cytotoxicity in compound libraries. Researchers can look for cytotoxic compounds, if they are interested in developing a therapeutic agent that targets cancer cells. Thebrine shrimp lethality assay is a method by which one can check the toxicity of the compounds on brine shrimp. The experiment was carried out following the protocol of Mayer *et al.*[XVII]Brine shrimp (*Artemia cysts*) eggs were hatched in a shallow rectangular plastic dish (22×32 cm), filled with artificial seawater, which was prepared with commercial salt mixture and double distilled water. An unequal partition was made in the plastic dish with the help of a perforated device. A set of 2,4,8,16,20 µg/mL in the test tube was prepared from a stock solution of 1000 µg/mL of the test compounds. The final volume in each test tube was adjusted to 2500 µL (1000 µL sea salt solution, 450µL double distilled water, 50 µL DMSO + complex and remaining 1000 µL were added as 10 nauplii in a sea salt solution). After 24 h number of dead nauplii were counted and from the survival % mortality was calculated.[XVIII,XIX]

2.5.5 Compounds interaction with biomolecule(DNA)

2.5.5.1 (a) Absorption titration spectroscopy

Electronic absorption titration was employed to study the relative binding mode of HS-DNA with molecules. The stock solutions of HS-DNA were prepared in phosphate buffer and stored at 4 °C for less than 4 days. The UV absorbance of HS-DNAat 260 and 280 nm in phosphate buffer (Na_2HPO_4/NaH_2PO_4, pH = 7.2) solution at room temperature gave a ratio of1.8-1.9:1, signifying that the DNA was suitably free fromproteins.[XX]The molar absorptioncoefficient of HS-DNA was taken as $12858M^{-1}cm^{-1}$. Absorptiontitration experiments were performed by maintaining constantcomplex concentration and varying the concentrationof HS-DNA. Complex-DNA solutions were allowed tobe incubated for 10 min at room temperature before measurements were taken. While measuring the absorption spectra, anequal quantity of HS-DNA was added to both the complex solution and the reference solution to eliminate the absorbance ofHS-DNA itself. A compound due to have anticancer activity binds the DNA in following distinct binding modes. (i) Electrostatic binding in which compound attacks the phosphate groups attached to DNA backbone on its external helical side. (ii) Groove binding in which compound attacks two grooves of DNA double helix and (iii) intercalation mode of binding in which compound is inserted between the stacked base pairs of DNA.[XXI]Upon interaction of compound with DNA, alteration arises in the helical structure of DNA. This causes hyperchromic effect and hypochromic effect

which are the spectral features of DNA concerning its double helix structure.The intrinsic binding constant K_b can be obtained using the following equation in literature.[XXII]

2.5.5.2 b) Viscosity measurements

Viscosity experiment was made using an Ubbelohde viscometer,engrossed in a water bath at 25.0 ± 0.5^{0}C. The viscosity of a 200 μM solution of HS-DNA was determined in the presence of the complexes using different [complex]/[DNA] ratios in the range of 0.00 to 2.00. The flow time was measured in triplicate with a digital stopwatch and then averaged. The relative viscosity ratio (η/η_o) was plotted against the r-bound (where η and η_o were the relative viscosity for DNA in the presence or absence of complexes, respectively).The hydrodynamic length of DNA generally increases upon partial intercalation while it does not lengthen upon groove binding.[XXIII] Viscosity measurements can sensitively detect the lengthening of a DNA helix induced by the binding of intercalatorsand thus provide evidence of intercalation for small DNA-binding molecules.[XXIV]The data are represented as the plot of the relative viscosity, i.e.($\eta/\eta_0)^{1/3}$vs.[complex]/[DNA].

2.5.5.3 (c) Molecular modeling assay

Docking study was made for Pt(II) complexes with biomolecule (DNA), to identify the binding mode of action and the vital functional groups interacting with the DNA, using Hex 8.0 software. Pt^{II} complexes were taken from their enhanced structure as a molecule and converted to .pdb (Protein Data Bank)format using CHIMERA 1.5.1 software. The change of transcription or replication of DNA may leading to gene mutation, thus causing a series of diseases, in this way it plays an irreplaceable role in life. DNA is also the target of many antibacterial drugs, antiviral, cancer and playing animportant role in the treatment of diseases.HS-DNA used in the experimental work was too large for current computational resources to dock, therefore, the structure of the DNA of sequence $d(ACCGACGTCGGT)_2$ (1BNA) is used for interaction study (PDB id: 1BNA, a familiar sequence used in oligodeoxynucleotide study) obtained from the Protein Data Bank (http://www.rcsb.org/pdb).[xxv] All calculations were done using on an Intel CORE i5, 2.5 GHz based machine running MS Windows 8, 64 bit as the operating system. The by default parameters were used for the docking calculation with correlation type shape only, FFT mode at 3D level, grid dimension of 6 with receptor range 180 and ligand range 180 with twist range 360 and distance range 40. The best conformation was selected with the lowest binding energy (kJ/mol).[XXVI]

2.5.5.4 (c) Fluorescence quenching analysis

Emission intensity measurements of ethidium bromide (EB = 3,8-diamino-5-ethyl-6-phenylphenanthridinium bromide) with free HS-DNA in the absence and presence of Pt(II) complexes were performed in phosphate buffer. The HS-DNA solution was up to the value of r = 3.33 ([DNA]/[Complex]) of pre-treated EB–DNA mixture ([EB] = 33.3 μM, [DNA] = 10 μM) at ambient temperature and incubate for 10 min before measurement. The emission intensity was recorded in the range of 500-800 nm. The emission intensities at 610 nm (λ_{max}) were obtained through excitation at 510 nm and slit wavelength 1.45 nm in the FluoroMax-4, HORIBA (Scientific) spectrofluorometer. The changes in fluorescence intensities of ethidium bromide and ethidium bromide bound to DNA were measured with respect to different concentration of the complex. The ethidium bromide has less-emission intensity in phosphate buffer solution 7.2 pH due to florescence quenching of free ethidium bromide by the solvent molecules. In the presence of DNA, EB exhibits higher intensity due to its partial intercalative binding mode to DNA.Fluorescence quenching of an EB-DNA can arise owing to inner-filter effect. The mechanism of quenching is found from the emission intensity of EB. In our study, inner filter effect was corrected with the following equation in this literature.[XXVII,XXVIII]

To examine the fluorescence quenching mechanism, the Stern–Volmer quenching constant (K_{sv})was determined by equation (1):[XXIX,XXX]

$I^0/I = Ksv[Q] + 1$(1)

where, I_0 and I are the emission intensity of EB-DNA in the absence and presence of quencher (complex), K_{sv} is the linear Stern-Volmer quenching constant obtained from the plot of I_0/I vs. [Q] and [Q] is concentration of quencher.To determine the strength of the interaction of complexes with DNA, the value of the associative binding constant (K_a) was calculated using the Scatchard equation (2):[XVIII,XXXI]

$log\ \mathrm{I_0} - \mathrm{I/I} = \log Ka\ + nlog[Q]$ (2)

where, I_0 and I are the fluorescence intensities of the EB-DNA in the absence and presence of different concentrations of complexes, respectively and n is the number of binding.The acting forces between drugs and biomacromolecules include hydrogen bonds, van der Waals forces, electrostatic attraction and hydrophobic interaction, etc. In order to estimate the interaction force of all compounds, the standard free energy changes (ΔG) for the binding process have been calculated using the Van't Hoff equation (3):[XXXII]

$\Delta G^0 = -RTlnKa$(3)

where, T is the temperature (25 ^{0}C, 298 K here), K_a is associative binding constant and R is gas constant 8.314 Jmol^{-1} K^{-1}. The negative sign for ΔG^0 means that the binding process is spontaneous.

2.5.6 DNA nuclease assay

Gel electrophoresis study was performed using pUC19 DNA with synthesized compounds. The samples were incubated for 0.5 h at 37℃. The samples were analysed by 1% agarose gel electrophoresis [Tris–acetate–ethylenediaminetetraacetic acid, (TAE) buffer, pH 8.0] for 3 h at 100 mV. The gel was stained with (0.5 mg mL^{-1}) ethidium bromide. The gels were viewed in an Alpha Innotech Corporation Gel doc system and photographed using a CCD camera. The cleavage efficiency of the compounds, the degree of DNA cleavage activity was measured by determining the ability of the complex to SC-DNA to OC-DNA equation describe in literature.[XXXIII]

3. Results and discussion

3.1 Magnetic moments, electronic spectral analysis and conductance measurements

The ambient temperature magnetic moments show that the Pt(II) complexes are diamagnetic in nature, which corresponds to the +2oxidation state of platinum metal ion, and are consistent with low-spin t_2g^6 eg^2 configuration for Pt(II) in square planar geometry. The UV-visible spectra of Pt(II) complexes(I-V) show strong vibrionic-structured bands within range of 241-355 nm, these series of intense transitions with ε in the order of 10^4Lmol^{-1}cm^{-1}. Absorption spectrum obeys the Lambert-Beer's law and concentration of compoundsare taken in the range of 100-150 μM.The electronic absorption spectral data are summarized in the experimental section. The high-energy absorption band at about 241-260 nm is due to as intraligand (IL) transitions of the quinazolinone based ligands designated as n–π* band and metal to ligand charge transfer (MLCT) bandof Pt(II) complexesis observed in between wavelength 320-355 nm designated as π–π* transitions. The low energy absorption band at about 349-351 nm region is assigned to the d–d transition.[XXXIV,XXXV] All Pt(II) complexes are soluble in solvent DMSO and non-electrolytic in nature ($\Lambda_m \leq$ 19-25 Ω^{-1}cm^{2}mol^{-1}).

3.2 ^{1}H NMR, ^{13}C NMR andFT-IR spectral analysis

The structural evidence of the synthesized Pt(II) complexes can be concluded from the ^{1}H NMR and ^{13}C NMR spectra and their relevant chemical shifts. The ^{1}H NMR spectra of the complexes and ligands are represented in supplementary material 1. The appearance of multiple peaks at 7.2-8.4 ppm suggests the presence of aromatic proton in the synthesized compounds. The aliphatic methyl protons observed at about 0.9-1.25 ppm. In ligand, carboxamide (N-H) proton peak is observed in the range of 9.6-10.14 ppm region, and thisproton peakis shifted to downfield regiondue to complexation (12.0-13.65 ppm), except that the peak due to the NH group resonance is absent. No other significant changes can be found in the other signals of the complexes.

In ^{13}C NMR spectra of ligands, the aromatic carbons are observed in between 112-136 ppm region.The imine(>C=N)group carbon peakobserved at 156 ppm and to be shifted downfield at about 159 ppm in the Pt(II) complexes. ^{13}C NMR spectra of the synthesized quinazolinone derivatives ligands and their complexesare shown in supplementary material 2.

The main aim behind subjecting the metal complexes toIR spectroscopyhas beeninterpreted as the functionalities present in the complexes formedalong by the conformation of the complexation involved betweenthe platinum metal and ligands.Infrared spectral data are represented in experimental section and supplementary material 3.The iminenν(C=N) group band of ligands are observed in the range of1611-1520 cm^{-1} to be shifted to higher frequency by *ca.* 50 cm^{-1}, indicating that the coordination of nitrogen with metal ion.The $\nu(>C=O)_{carboxamide}$ band ofligands is observed in betweenregion 1630 to 1650 cm^{-1}and is shifted to higher frequency by *ca.* 30 cm^{-1},on complexation.The metal nitrogen bondν(Pt-N) is observed at 550 -578 cm^{-1} and themetal-sulphur bond ν(Pt-S) is observed in the region 625-633 cm^{-1}.

3.3 LC-MS analysis

The LC-MS spectrum and possible mass fragmentation pattern of mononuclear Pt(II) complex (V) is represented in Figure 1.The mass spectra and mass fragmentation of the ligands (L^1-L^5) are represented in supplementary material 4 and mass spectral data of the ligands (L^1-L^5) are represented in experimental section. The mass spectrum of the complex (V) shows molecular ion peaks [M], [M+2], [M+4], at 487.98 m/z, 489.97m/z and 491.98 m/z, respectively, due to the presence of two chlorine atoms. The peak at 418.01 m/z is due to the loss of two chlorine atoms. The peak at 223.07 m/z is due to the loss of the platinum metal ions and remaining ligand. The peak at 146.05 m/z is due to the loss of the pyridine ring corresponds to the quinazolinone nucleus.

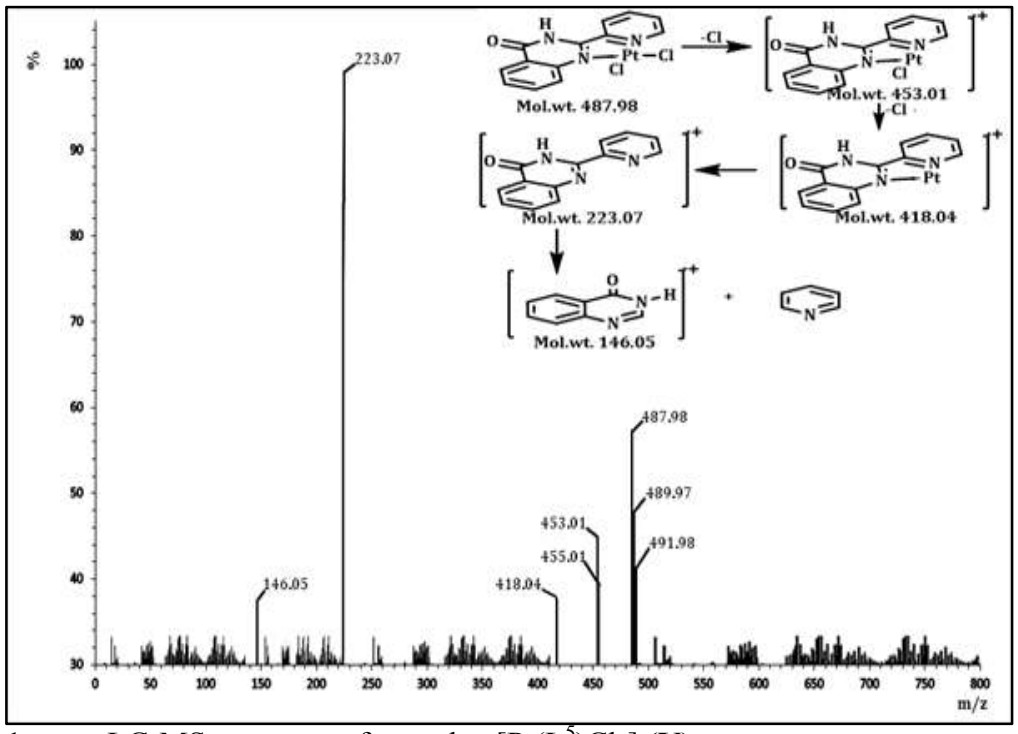

Fig. 1 LC-MS spectrum of complex $[Pt(L^5)Cl_2]$ **(V)**

3.4 Thermal property (TGA)

The thermal property of mononuclear Pt(II) complex (V) was characterized by thermal gravimetric analysis (TGA) under nitrogen (N_2)atmosphere and is represented in supplymetry material 4. The Pt(II) complexes decomposed in two steps.[XXXVI] In the first step, weight loss occurs between 180 - 220 ^{0}C (14%), which is attributed to the loss of two chlorinemolecule and in second step, decomposition occursin the range of 240 - 430 ^{0}C, which is attributed to the loss of ligand (weight loss of 46%), and leaving behind residue as platinum metal ion.[XXXVI]

3.5 Biological application

3.5.1 In vitro antimicrobial assay

The antimicrobial activities of the synthesized compounds were tested against randomly selected three Gram$^{(-ve)}$and two Gram$^{(+ve)}$bacterial strains. Some of the platinum(II) complexes containingelectron withdrawing functional group show high IC_{50} values against electron releasing group. All the Pt(II) complexes 29-90µM exhibit significant antibacterial activities compared to free ligands 100-280µM and metal salt(Figure 2).Such increased activity of the complexes can be explained on the basis of overtone's concept and the Tweedy's chelation theory.[XXXVII]The mechanism of antimicrobials may contain different targets in a microorganismthat can cause disease, e.g. destruction to the cytoplasmic membrane, interfering with cell wall and, the inhibition of energy production (APT). The increase in antimicrobial activity of complexes can be the result of: (I) nature of the ion neutralising the complex, (II) chelate effects, (III) nuclearity of the metal centre in the compounds and (IV) nature of the ligands. The inhibition activity seems to be governed in certain degree by the facility of coordination at the metal centre as well as electronic nature of the ligands.[XXXVIII]The result of MIC in terms of µM are represented in the supplementary material5. From the result, it is concluded that all the Pt(II) complexes exhibit moderate to good activity against all the five microorganism as compared to ligands.

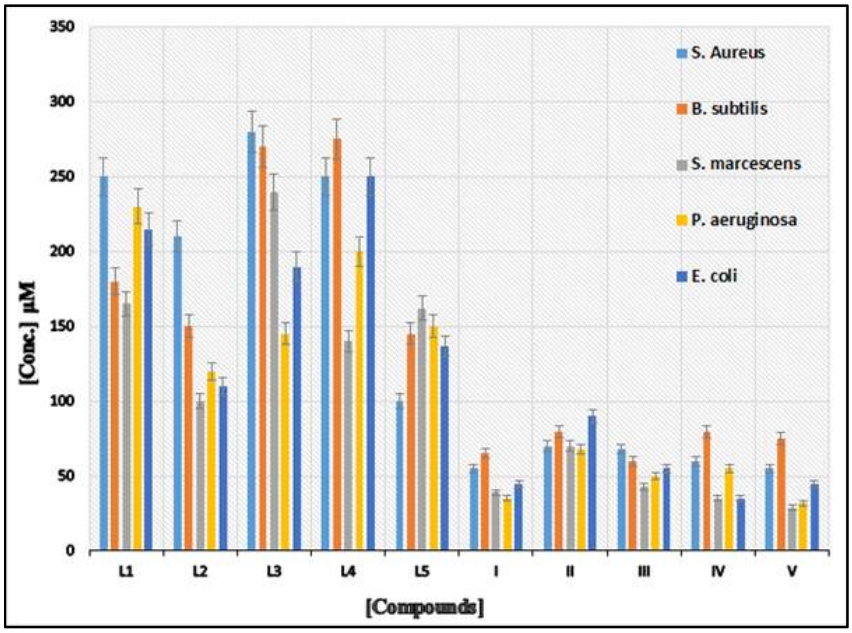

Fig. 2. Effect of different concentrations of free ligands and synthesized complexes on five different microorganisms. Error bars represent the standard deviation of three replicates.

3.5.2 Cellular level bioassay using S. pombe cells

Due to eukaryotic and fairly big size of *S. pombe*, it has become an important tool to study cell biology. Cellular levelcytotoxicity of synthesized compounds was tested against*S. pombe* cells.[XXXIX]Complexes (I-V) aremore toxic than quinazolinone derivatives ligands (L^1-L^5), while the cisplatin and transplatin are found to be more cytotoxicas compared to complexes (Figure 3). Cytotoxicity data of all compounds are shown in supplementary material 6.After 17-20 h of the treatment, many of the *S. pombe* cells are destroyed due to lethal nature of the compound.

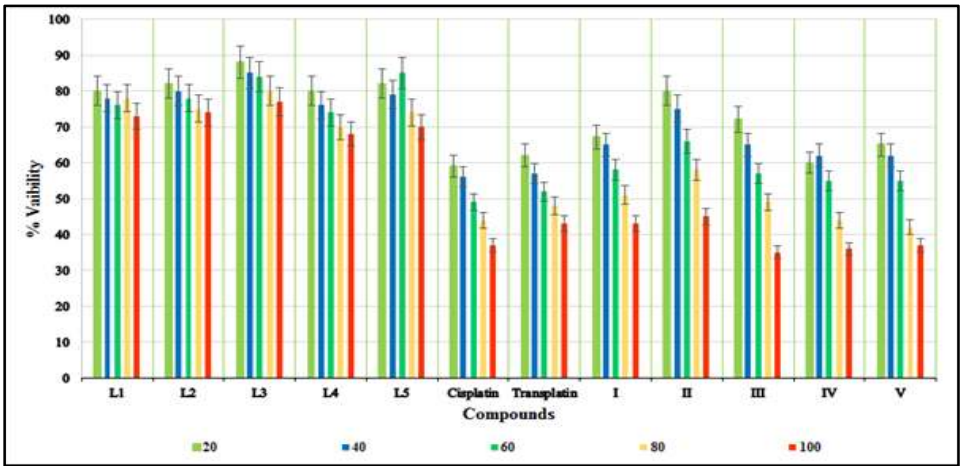

Fig. 3. Effect of compounds on percentage viability of *S. pombe* at different concentration.

3.5.3 In vitro cytotoxicity bioassay

The mortality rate of nauplii is found to increase with increasing concentration of sample. LC_{50}value of complexesarein the range of 6.74-11.70 µg/mL and the LC_{50}value of the ligands

are in the range of the 77.62-100.0 µg/mL (Figure 4).The percentage mortality of brine shrimp nauplii are calculate from the number of dead nauplii.From the result it is inferred that the 50 percentage lethal concentrations (LC_{50})of cisplatin, transplatin and platinum(II) complexes exhibit significanttoxicity as compared to synthesized ligands against brine shrimp and can be further studied *in vivo* for their anticancer property.

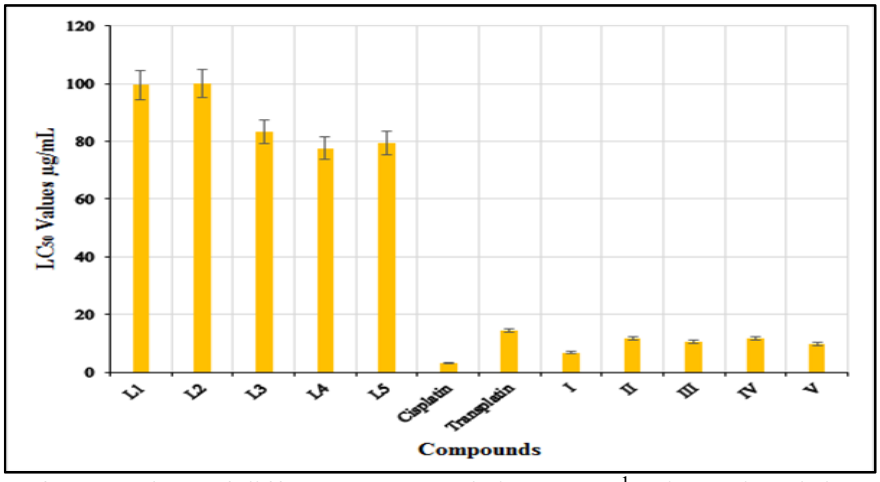

Fig. 4. Plot of LC_{50} values of different compounds in µg mL^{-1} using Brine shrimp. Error bars represent the standard deviation of three replicates.

3.5.4 Mycobacterium tuberculosis (Mtb) H_{37}Rv strain

Antituberculosisscreening of the complexes (I-V) were conducted at250 µg/mLconcentrations against*Mycobacterium tuberculosis*H_{37}Rv strain. Complex **II** (5-NO_2)has been found to possess excellent activity against *Mycobacterium tuberculosis* H_{37}Rv strain.Compound **V** (-Py) and **IV** (Benzo[b]thiophene)are moderately active and remaining all other compounds exhibit poor inhibition against *M. tuberculosis* H_{37}Rv growth.Isoniazid and rifampicin are used as the referencedrugs. The compounds which exhibit higher inhibition against *M. tuberculosis* H_{37}Rv, are further screened for theMIC. The IC_{50} values of synthesized complexes are in the order of Rifampicin > Isoniazid >II>V>IV>I>III and are represented in Figure 5.

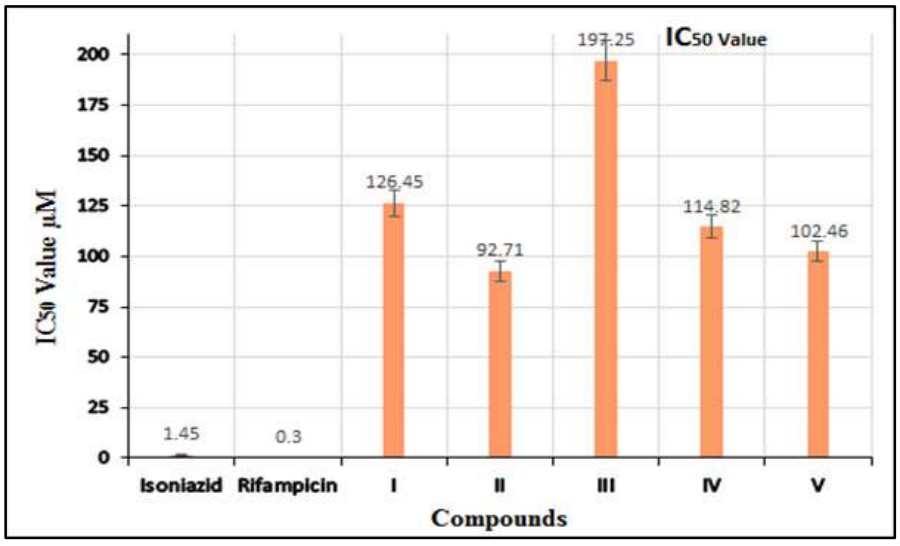

Fig. 5. Tuberculosis assay of synthesized complexes (I-V).

3.5.5 General structure–activity relationship (SAR)

The significances of the biological evaluation revealed that the activity is significantly affected by introducing R_1 (-H, -CH_3) at C-3'(position-3) in thiophene ring, R_2 (-NO_2) at C-5' (position-5) in thiophene ring, benzo[b] thiophene ring at C-2 position and pyridine ring at C-2 position in quinazolinone moiety (Figure 6).It is observed that the complexes**(II, IV, V)** containing electron withdrawing group (-NO_2, benzo[b] thiophene, pyridine)on quinazolinone nucleus exhibit excellent anti-tuberculosis activity against*Mycobacterium tuberculosis* (Mtb) H_{37}Rv strain.The presence of electron donating group -CH_3**(III)** as at C-3' (position-3) in thiophene ring **(I)**show moderate anti-tuberculosis activity against *Mycobacterium tuberculosis (Mtb)* H_{37}Rv strain.The presence of electronwithdrawinganddonating group involving complexes such as **(I), (II), (III), (IV)** and**(V)** are established superior antibacterial activity against Gram$^{(+ve)}$and Gram$^{(-ve)}$ micro-organism(*Bacillus subtilis*, *Staphylococcus aureus,Escherichia coli,Pseudomonas aeruginosa*and *Serratia marcescens*). The complexes(**I, III, IV**) containing electron withdrawing groupare more potent against *S. Pombe* cells in *in vitro*cellular levelcytotoxicity andagainst *Artemia cyst* in brine shrimp lethality bioassay as compared to other complexes **(II, V)**containing electron releasing group.

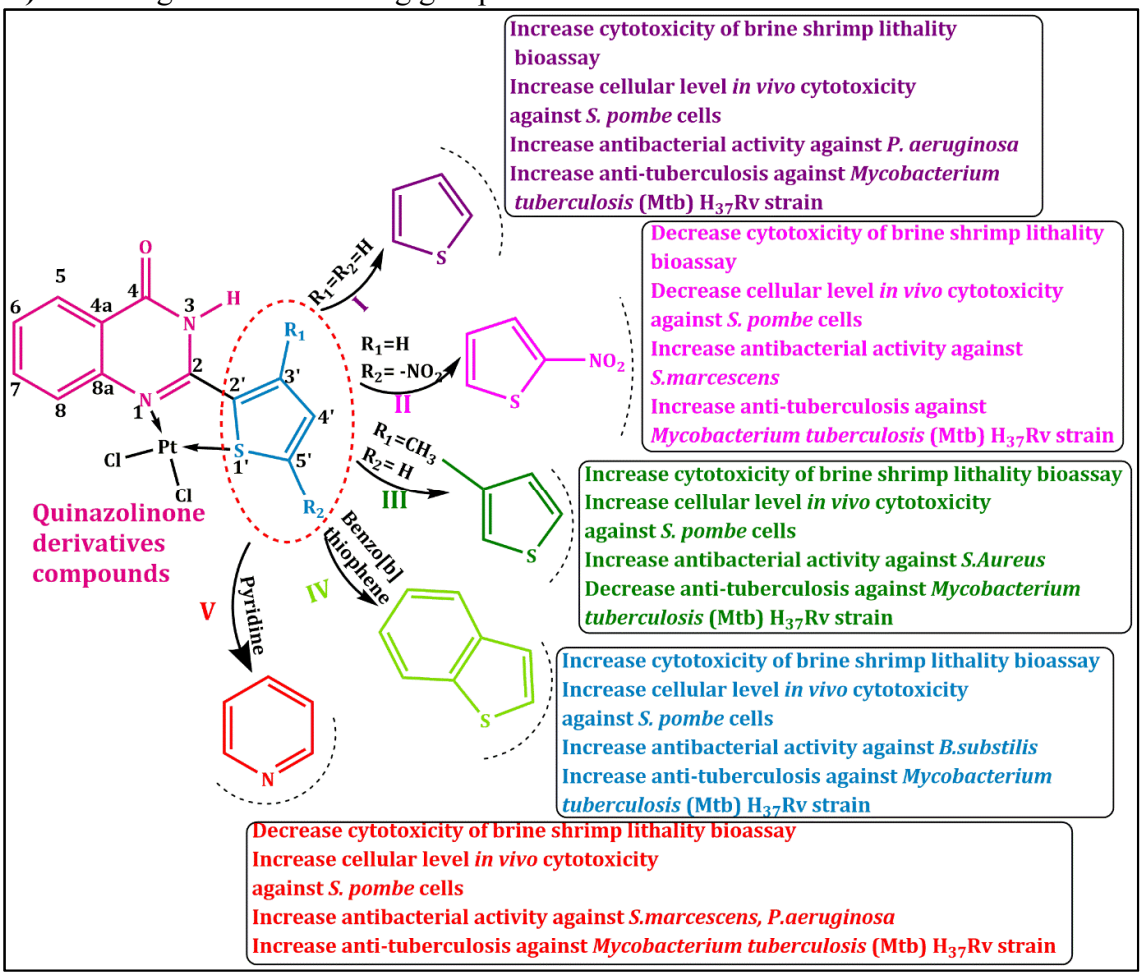

Fig. 6. Structure–activity relationships (SAR) for antimicrobial, antituberculosis and cytotoxicity activity, cellular level cytotoxicity of the synthesized complexes (I - V).

3.5.6 DNA interactions studies.

3.5.6.1(a) By electronic absorption titration

The interaction of platinum(II) complexes with DNA was studied using UV-Vis absorption titration spectroscopy in order to get some information about their binding mode.In Figure 7, the absorption spectrum of platinum(II) complexes**(I-V)**in the presence of increasing amount of HS DNA with a decrease absorption intensity (hypochromism) and 1-3 nm wavelength slightly red shifted, from this graphsit concluded that the complexes binds with DNA via partial intercalation mode. The compound binds to DNA through external interaction, the absorption bands are observed in at 310 nm revealedsignificant and red shift was owing to the participation of aromatic chromophores in hyperchromic effect. The charge transfer bands are slightly red shift indicative of the partial intercalative mode of binding. Since, DNA takes several hydrogen- bonding sites which are available both in major and minor grooves.

The K_b values for the platinum(II) complexes **(I-V)** are observed in the range of 1.11×10^5–$6.81 \times 10^5 M^{-1}$. The percentage hypochromicity (*H*%) are observed in range of17.46-28.27%with an increasing volume of HS-DNA,indicating the partial intercalative mode of binding. The complex **(V)** show highK_b value due to presence of N, N-donor ligand containing pyridine (Py) ring, while lower thanclassical intercalator EB ($K_b = 4.94 \times 10^5 M^{-1}$).[XL]Binding constant ($K_b$) of synthesized complexes are found higher than that of carboplatin ($0.33 \times 10^3 M^{-1}$) and oxaliplatin ($5.3 \times 10^5 M^{-1}$).[XLI]The DNA binding interaction are further examined by a viscometric technique and fluorescence quenching analysis. The binding affinity gradually decreasing with the electron withdrawing group of the complexes, and the order of complexes are V>II>IV>I>III.

The thermodynamics parametersof complexes and ligands were calculated using the Van't Hoff equation (5).[XLII]

$$ln\, Kb = \frac{\Delta H^{\circ}}{RT} + \frac{\Delta S^{\circ}}{R} (5)$$

$$\Delta G = \Delta H^{\circ} - T\Delta S^{\circ} \quad (6)$$

where,binding constantis at the analogous temperature (T)and R is the gas constant. The Van't Hoff plots for complex-DNA interaction are shown in Figure8.The enthalpy change (ΔH^0) is calculated from the slope of the Van't Hoff relationship and entropy change (ΔS^0) from the intercept. The Gibb's free energy change (ΔG^0) is calculated from equation (6) at T = 298, 301, 303, 308 and 313 K.[XLIII]Binding constants (K_b)values at different temperature and thermodynamics parameters are the measure of the complex–DNA stability. While the free energy indicates the spontaneity of complex–DNA binding. Moreover, the K_b is decrease with the increase temperature.The thermodynamic parameters of the platinum(II) complexes**(I-V)**are negative, it indicate that the spontaneity of complex–DNA interaction (Table 1).

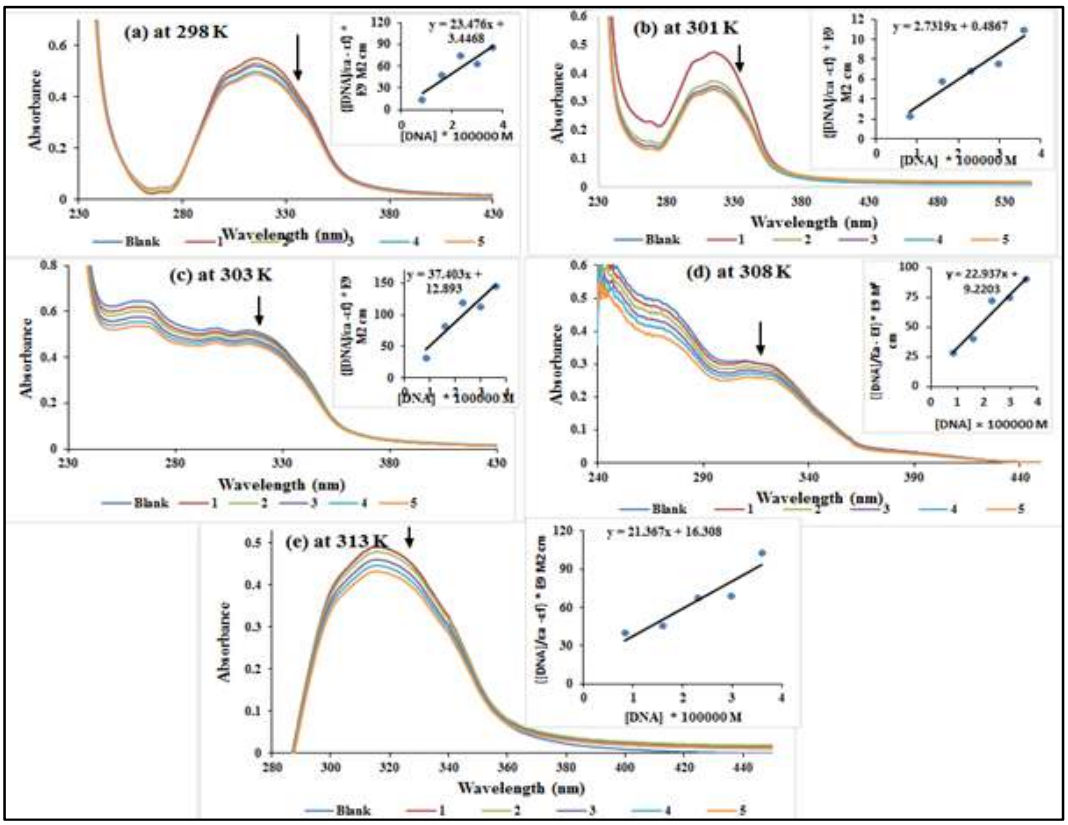

Fig. 7. Concentration spectral changes upon addition of HS DNA to the solution of complex (V) after incubating it for 10 minutes at different temperature (a) at 298 K (b) at 301 K (c) at 303 K (d) at 308 K (e) at 313 K in phosphate buffer (Na_2HPO_4/NaH_2PO_4, pH = 7.2). Inset: plot of [DNA]/ (εa-εf) *vs*. [DNA].

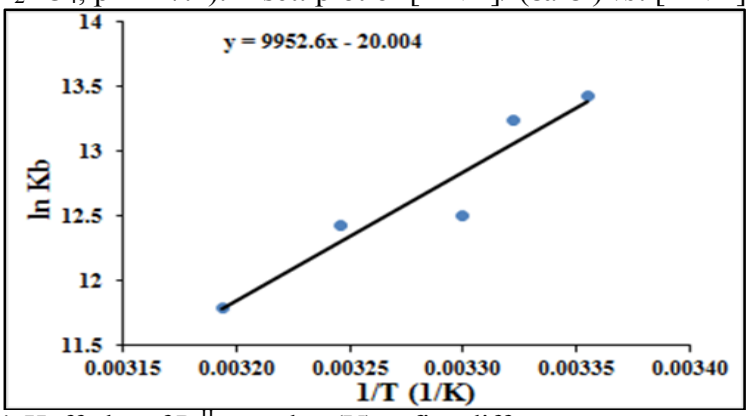

Fig. 8. The Van't Hoff plot of Pt^{II} complex (V) at five different temperatures.

Table 1. The binding constant (K_b) and thermodynamic parameters for the interaction of Pt^{II} complexes with DNA at five different temperatures.

Compounds	λ_{max} (nm)		Δλ (nm)	T (K)	$K_b \times 10^5$ (M^{-1})	Hyper. (%)	ΔH (kJ mol^{-1})	ΔS (J mol^{-1} K^{-1})	ΔG (J mol^{-1})
	Bound	Free							
I	289	284	5	298	2.17	18.97	-1823	-40.909	-6,047.53
	313	312	1	301	2.07	19.34			-5,924.80

	313	312	1	303	2.00	17.46			-5,842.98
	313	312	1	308	1.61	17.92			-5,638.44
	313	312	1	313	1.59	18.36			-5,433.89
II	317	315	2	298	3.82	18.96	-3784	-20.366	-31,775.1
	311	310	1	301	3.17	18.09			-31,714.0
	312	311	1	303	2.61	18.33			-31,673.3
	313	314	1	308	2.54	18.05			-31,571.5
	311	312	1	313	1.70	18.45			-31,469.6
III	306	305	1	298	2.58	18.28	-4708	-54.882	-30,730.5
	306	305	1	301	1.86	18.18			-30,565.9
	262	259	3	303	1.62	24.01			-30,456.1
	288	285	3	308	1.59	17.46			-30,181.7
	313	312	1	313	0.89	18.69			-29,907.3
IV	307	306	1	298	3.07	18.69	-4669	-51.935	-31,218.1
	262	260	2	301	2.20	18.75			-31,062.3
	308	305	3	303	2.17	20.05			-30,958.4
	307	305	2	308	1.85	19.61			-30,698.7
	265	263	2	313	1.11	19.54			-30,439.0
V	316	315	1	298	6.81	17.90	-8274	-166.31	-33,184.5
	315	314	1	301	5.61	28.27			-32,685.6
	315	314	1	303	2.87	17.47			-32,353.0
	303	301	2	308	2.48	18.75			-31,521.4
	317	316	1	313	1.31	17.84			-30,689.8

Hyper.(%) = $[(A_{free} - A_{bound})/A_{free}] \times 100\%$, K_b = Intrinsic DNA binding constant determined from the UV-Vis absorption spectral titration, T = Temperature in kelvin (K), ΔH = Change in enthalpy, ΔS = Change in Entropy, ΔG = Gibb's free energy, Δλ = Difference between bound wavelength and free wavelength.

3.5.6.2(b) By viscosity measurements

The viscosity measurements is most critical and least uncertain tests of a binding in solution in the absence of crystallographic data. No increase in the axial length of the DNA is generally observed for a groove binding and therefore did not alter the relative viscosity.[XLIV,XLV] In contrast, cisplatin can bend DNA through covalent binding resulting into shortening of the axial length of the double helix, caused a decrease in the relative viscosity of the solution.[XLVI] Partial intercalators also reduce the axial length observed as a reduction in relative viscosity, whereas the classical organic intercalators such as ethidium bromide increased the axial length of the DNA and it becomes more rigid,[XLIV,XLV] resulting in an increase in the relative viscosity. Here in our study, the relative viscosity measurement graphisshown in Figure 9. The order of increasing viscosity isV>II>IV>I>III, which ispresented to binding constant value (K_b).The hypochromic, bathochromic shifts and increasing viscosity suggest the partial intercalation mode of binding of complexes.

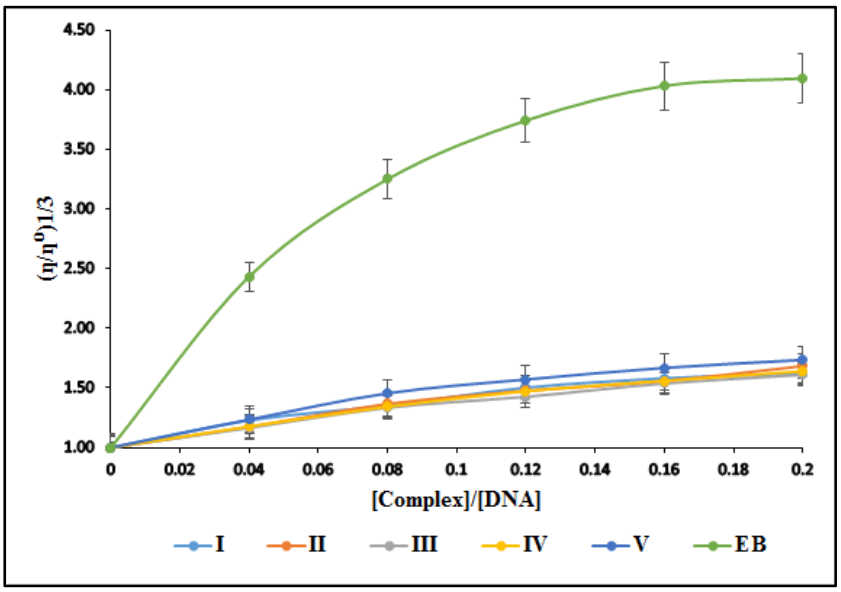

Fig. 9. The effect of increasing amounts of complexes (I - V) on the relative viscosity of HS DNA at 27 (±0.1) ^{0}C in phosphate buffer at pH = 7.2. Error bars represent the standard deviation of three replicates.

3.5.6.3 (c)ByMolecular docking with DNA

Thepossible binding site, interaction mode and binding affinity ofmoleculecan be determined by molecular docking study. In which complexes are docked to sequencedd(CGCGAATTCGCG)2 dodecamer B-DNA (PDB ID: 1BNA). The resulting model showed that compound recognizes DNA in the minor groove via intercalation interaction, which is situated within the G-C rich region from chain, through the planarity of quinazolinone core is comfortable for strong $\pi-$stacking interactions and fits inside the DNA strands by Van der Waals interaction and hydrophobic contacts.[XIV]Docking structure of compounds are shown in supplementary material7.Most stable binding conformation of complex **(V)** and DNA revealed that it is stacked in the minor groove.[XLVII,XLVIII]The molecular structures ofligand **(L^1-L^5)** and complexes **(I-V)** with B-DNA showedrelative binding affinity (-198.45 **(L^1)**, -221.66 **(L^2)**, -193.14 **(L^3)**, -201.98 **(L^4)**, -237.26 **(L^5)**, -226.58 **(I)**, -249.54 **(II)**, -226.54 **(III)**, -235.65 **(IV)**, -252.51**(V)** kJM^{-1}) indicating that complex **(V)**have better binding capability relative to other complexes under study, that is represented in Figure 10. The results of complexes (I-V) are compared with the UV-vis absorption titration, viscosity measurements and fluorescence quenching analysis study.

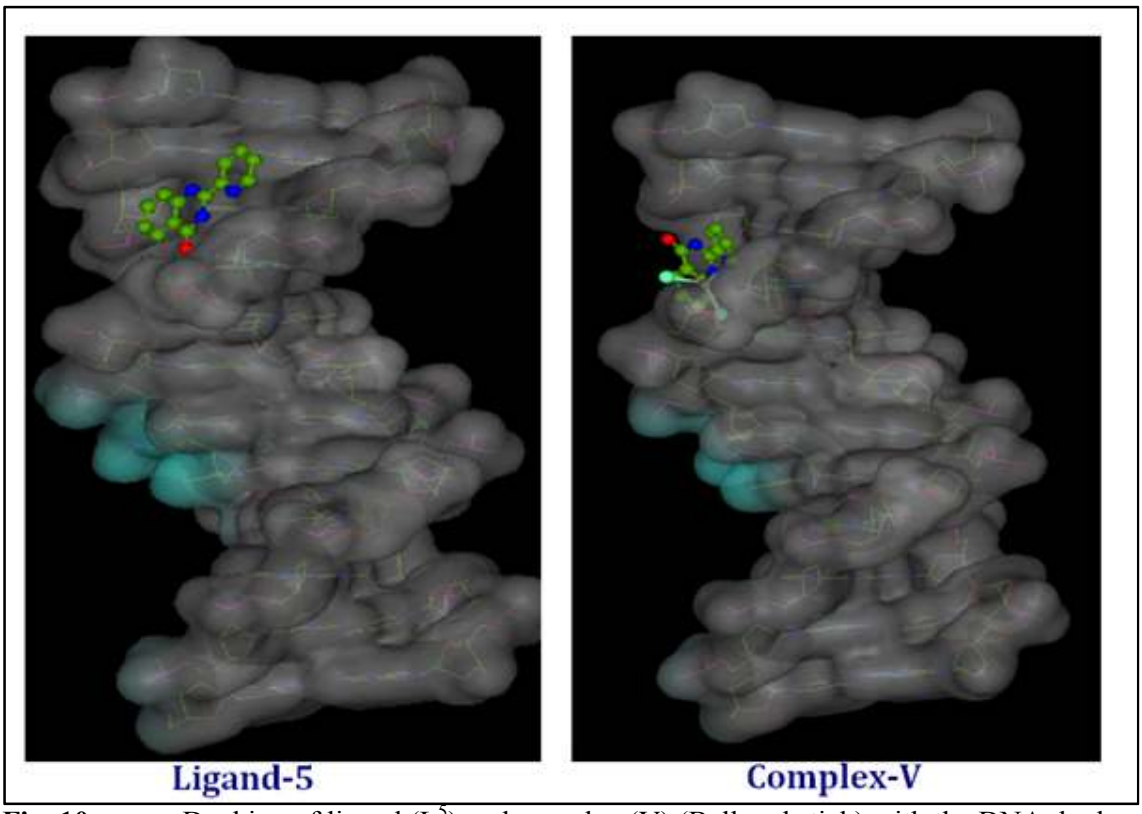

Fig. 10. Docking of ligand (L^5) and complex (V) (Ball and stick) with the DNA duplex (VDW spheres) of sequence d(ACCGACGTCGGT)$_2$. The compounds are docked into the DNA, showing partial intercalation between the DNA base pairs.

3.5.6.4(d) Fluorescence quenching analysis

In fluorescence quenching study, ethidium bromide (EtBr) as a cationic dye that is normally used forDNA interactionvia intercalation. Upon EB-DNA interaction, characteristic of EtBr shows the changes in absorbance, reflected by an enhancement in fluorescence intensity by about one order of magnitude, as compared to free dye in solution. Hence, when a platinum(II) complexes are added to the EB-DNA system, any quenching of the fluorescence will indicate the replacement of EB by the coordination molecule (DNA), via intercalative mode, it is expected of its strong stacking interaction between the adjacent DNA base pairs.

Fluorescence quenching analysis has been carried out for platinum(II) complexes and the corresponding emission spectra of the EB-DNA solutions in the presence of the increasing amounts of complex concentrations (r = 0.33 to 3.33), florescence quenching data of all complexes and graph are represented insupplementary material8. Which clearly indicate a dramatic increase in the fluorescence intensity of the EB-DNA by adding the Pt(II) complex. In DNA-EB system, the increase of the fluorescence intensity is due to releasing free EB molecules.Therefore, the formation of complex–DNA stops the binding of EB and the complete metal complex–DNA formation occurs when the study fluorescence intensity is sufficient.[XVIII]

Moreover, the Stern-Volmer quenching constants (K_{sq}), number of binding sites (n), change in standard Gibb's free energy (ΔG^0) and associative binding constant (K_a) data are

listed in Table 2, while the corresponding plots obtained from the experimental quenching data for the complexes are shown in Figure 11.

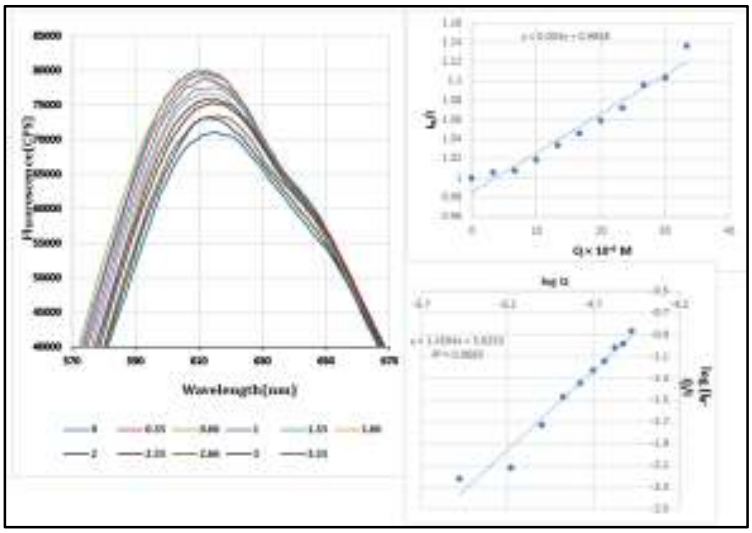

Fig. 11 Fluorescence emission spectra of EB bound to HS-DNA in the presence of complex (V). [EB] = 33.3 μM, [DNA] = 10 μM; [complex] = (i) 3.33, (ii) 6.66, (iii) 10, (iv) 13.33, (v) 16.66, (vi) 20, (vii) 23.33, (viii) 26.66, (ix) 30, (X) 33.3 μM; λ_{ex}= 510 nm. The arrows show the intensity changes upon increasing the concentrations of complex. Inset graph: plots of I_0/I *versus* [Q], with • for the experimental data points and the full line for the linear fitting of the data. Comparative plot of log[I_0-I/I] *versus* log[complex] for the titration of HS-DNA EB system with complexes (V) in phosphate buffer medium.

Table 2 Linear Stern-Volmer quenching constants (K_{sq}), Number of binding sites (n), change in standard free energy (ΔG^0) and associative binding constant (K_a) of Pt^{II} complexes (I-V)

Complexes	K_{sq} (M^{-1})	K_a (M^{-1})	n	ΔG(J mol^{-1})
I	2.9×10^3	0.47×10^4	1.049	-20,986.30
II	4.0×10^3	4.2×10^5	1.459	-32,091.30
III	1.1×10^3	0.80×10^3	1.009	-16,716.26
IV	5.2×10^3	1.03×10^5	1.305	-28,612.50
V	4.6×10^3	7.94×10^5	1.501	-33,658.40

with HS-DNA.

3.5.7 Gel electrophoresis

Figure 12 shows the cleavage of pUC19 DNA in presence of test compounds. The bands of the DNA control, K_2PtCl_4 salts, cisplatin, transplatin and complexes (I-V),indicate that thelanes1-9, respectively. DNA control lane shows two bands corresponding to supercoiled form (Form I) and open circular form (Form II). Lane 2(K_2PtCl_4 + DNA) also shows two bands, but the intensity of supercoiled form is different from that of control. Lane 3-9 (cisplatin, transplatin and complexes**(I-V)** + DNA) shows, 2 bands indicating a significant cleavage of DNA by the test complexes in reference to parent compound K_2PtCl_4 salts, cisplatin, and transplatin. Aquantitative measure of the DNA cleavage in terms of % cleavage for the test compounds is represented in the Figure 13 and tableis given in supplementary

material9. As the complexesshow DNA cleaving abilitysimilar to cisplatin, it can be concluded that thecomplexes inhibit the growth of the microorganismsby cleaving the DNA.

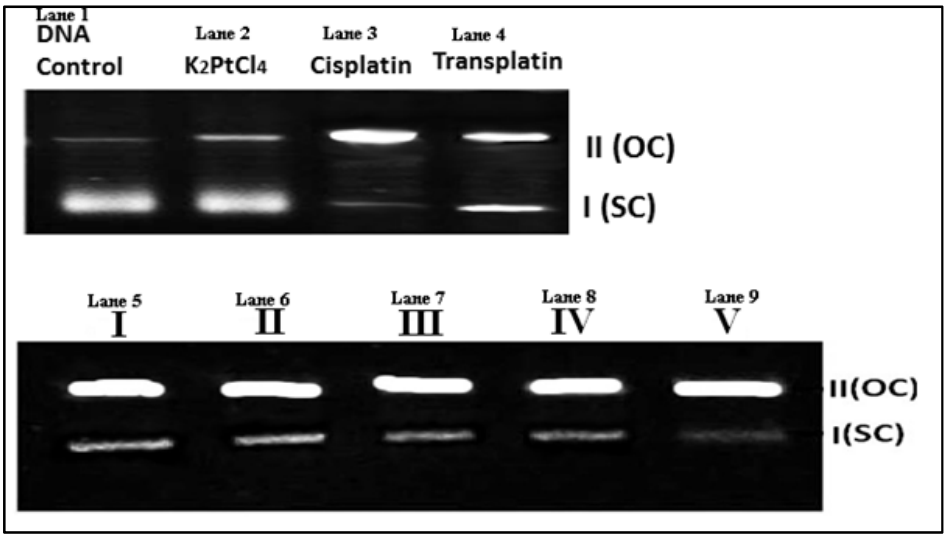

Fig. 12. Photogenic view of the cleavage of pUC19 DNA (300 µg/mL) with a series of compounds using 1% agarose gel containing 0.5µgml^{-1} EtBr. All reactions were incubated in TE buffer (pH 8) at a final volume of 15 mm^3 for 3 h at 37°C.

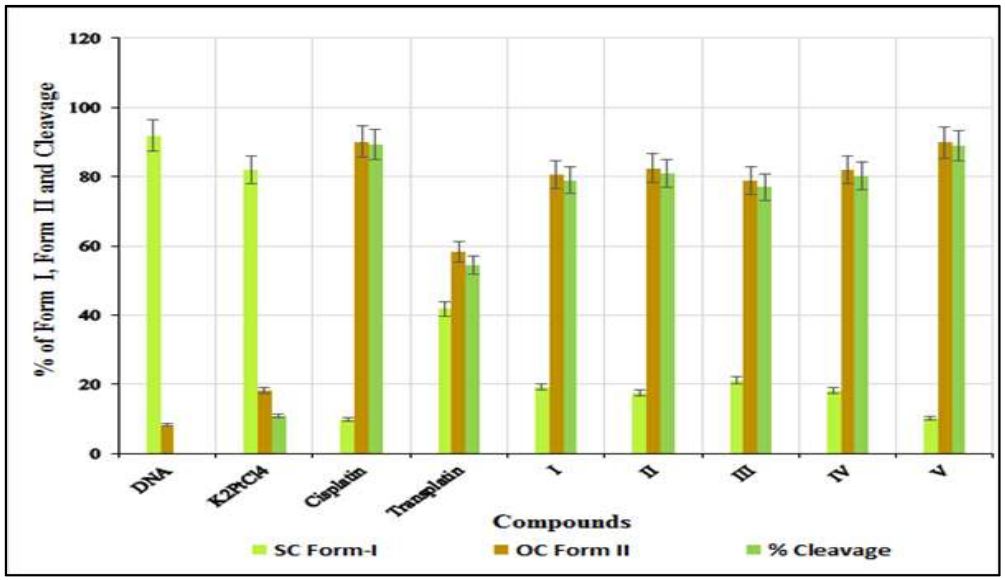

Fig. 13. Plot of DNA cleavage data by agarose gel electrophoresis of different compounds using pUC19 DNA. Error bars represent the standard deviation of three repeats.

Conclusion

In this current work, synthesis of different heterocyclic based platinum(II) complexes from the quinazolinone derivatives based ligands were studied. The synthesized compounds were spectroscopic characterized using ^{1}H NMR, ^{13}C NMR, FT-IR, TGA, mass, micro-elemental analysis and UV-vis techniques, and physicochemicallycharacterization using magnetic moments and conductance measurement. The micro-elemental analyses agree to the platinum metal: quinazolinone derivatives ligand stoichiometryof 1:1 mole ratio.The conductance

value of the platinum(II) complexes in DMSO solvent, exhibitedthat all complexes are non-electrolytic in nature. The FT-IR dataof the synthesized compounds werecarried out. The magneticmoments of the complexes reveal that they are all diamagnetic nature. It proposes thatplatinum (Pt) is in the +2 oxidation state due to formation complexation. The electronic spectral data suggest that all thecomplexes were found to have square planar geometry. In ^{1}H NMR spectra, the integral intensity of the (N-H) signal of free ligands and complexes are found to be in between 9 to 10 ppm and 12 to 14 ppm, respectively.The ^{13}C NMR spectra of ligands and complexes, the signal of (C=N) groupare detected156.00 ppm and 159.00 ppm, respectively. The biologically elucidation is also carried out for all newly synthesized compounds, interaction of the complex analogue with DNA was examined using electronic absorption titration, viscosity measurements, molecular modeling and fluorescence quenching analysis. All DNA binding studies prove that the interaction between complexes analogue and DNA through partial intercalativemechanism.Complex (V) is a higher binding ability than other complexes, because of the bidentate N,/N-donor ligand present.The maximum binding ability of N,/N-donor ligands as compared to N,/S-donor ligands. The DNA nuclease investigate have been carried out on the interaction of the complexes with DNA by gel electrophoresis technique. The results propose that high efficient cleavage of supercoil pUC19 DNA is obtained for all the complexes compared to the K_2PtCl_4 salt.Gel electrophoresis were carried out to the cisplatin and transplatin, the interaction of the drugs with DNA and, percentage cleavage ability of the cis-platin is higher than all complex and transplatin.All the synthesized compounds were established for their *in vitro* antimicrobial activity, *Mycobacterium tuberculosis* (Mtb) $H_{37}Rv$ strain and *in vitro* cytotoxicity and cellular level cytotoxicity and can be further explored for *in vivo* cytotoxicity studies against cell lines. The MIC values against the growth of microorganisms are much larger for platinum complexes than the free ligand and metal salt.Therefore,theDNA-binding and the cytotoxicity may be considered likely for any potential biological application as metallodrugs.

Declaration of interest

The authors report no conflicts of interest. The authors alone are responsible for the content and writing of the paper.

Acknowledgements

The authors thankful to the Head, Department of Chemistry, Sardar Patel University, Vallabh Vidyanagar, Gujarat, India, for providing the laboratory facilities, DST-PURSE, Sardar Patel University, Vallabh Vidyanagar for mass spectra analysis, P.G. Department of Bioscience, Vallabh Vidyanagar, Gujarat, India, for providing the biochemistry laboratory facilities, to carried out cellular level cytotoxicity and gel electrophoresis techniques. Dhanji P. Rajani, microcare laboratory, Surat for *in vitro* antituberculosis activity, U.G.C., New Delhi for providing financial assistance of a UGC BSR grant no. C/2013/BSR/Chemistry/7489 and "BSR UGC One Time Grant", vide UGC letter no. F.19-119/2014(BSR).

References

I. B. Rosenberg, L. Vancamp, J.E. Trosko, V.H. Mansour, Platinum Compounds: a New Class of Potent Antitumour Agents, Nature, 222 5191 (1969) 385-386.

II. M.S. Malamas, J. Millen, Quinazolineacetic acids and related analogs as aldose reductase inhibitors, Journal of Medicinal Chemistry, 34 4 (1991) 1492-1503, doi: 10.1021/jm00108a038.

III. O.M.M. Habib, E. B.; Girges, M. M.; El-Shafei,, A. M. Boll. Chim. Farm. , 134 (1995, ,) 503.

IV. A.K. Mannscherck, H.; Stuhler, G.; Davis, M. A.; Traber, , J.Eur. J. Med. Chem, 19, (1984,) 381.

V. N.J. Liverton, D.J. Armstrong, D.A. Claremon, D.C. Remy, J.J. Baldvin, R.J. Lynch, G. Zhang, R.J. Gould, Nonpeptide glycoprotein IIb/IIIa inhibitors: Substituted quinazolinediones and quinazolinones as potent fibrinogen receptor antagonists, Bioorganic & Medicinal Chemistry Letters, 8 5 (1998) 483-486, doi: http://dx.doi.org/10.1016/S0960-894X(98)00047-X.

VI. J.B. Jiang, D.P. Hesson, B.A. Dusak, D.L. Dexter, G.J. Kang, E. Hamel, Synthesis and biological evaluation of 2-styrylquinazolin-4(3H)-ones, a new class of antimitotic anticancer agents which inhibit tubulin polymerization, Journal of Medicinal Chemistry, 33 6 (1990) 1721-1728, doi: 10.1021/jm00168a029.

VII. S. Kobayashi, M. Ueno, R. Suzuki, H. Ishitani, Catalytic asymmetric synthesis of febrifugine and isofebrifugine, Tetrahedron Letters, 40 11 (1999) 2175-2178, doi: http://dx.doi.org/10.1016/S0040-4039(99)00142-2.

VIII. R.A. LeMahieu, M. Carson, W.C. Nason, D.R. Parrish, A.F. Welton, H.W. Baruth, B. Yaremko, (E)-3-(4-oxo-4H-quinazolin-3-yl)-2-propenoic acids, a new series of antiallergy agents, Journal of Medicinal Chemistry, 26 3 (1983) 420-425, doi: 10.1021/jm00357a018.

IX. L.B. Fisnerova, B.; Kocfeldova, Z.; Tikalova, J.; Maturova, E.; Grimova,, Collect. Czech. Chem. Commun 56 (1991) 2373.

X. E. Rodriguez Arce, M.F. Mosquillo, L. Perez-Diaz, G.A. Echeverria, O.E. Piro, A. Merlino, E.L. Coitino, C. Maringolo Ribeiro, C.Q.F. Leite, F.R. Pavan, L. Otero, D. Gambino, Aromatic amine N-oxide organometallic compounds: searching for prospective agents against infectious diseases, Dalton Transactions, 44 32 (2015) 14453-14464, doi: 10.1039/C5DT00557D.

XI. B.E. Smart, Fluorine substituent effects (on bioactivity), Journal of Fluorine Chemistry, 109 1 (2001) 3-11, doi: http://dx.doi.org/10.1016/S0022-1139(01)00375-X.

XII. M.R.K. ElhamJafari, Res Pharm Sci., 11 1 (2016) 1-14.

XIII. K.D. Hodges, J.V. Rund, Oxidative addition of halogens and pseudohalogens to dihalo(1,10-phenanthroline)platinum(II), Inorganic Chemistry, 14 3 (1975) 525-528, doi: 10.1021/ic50145a015.

XIV. M.V. Lunagariya, K.P. Thakor, B.N. Waghela, F.U. Vaidya, C. Pathak, M.N. Patel, Design, synthesis, MTT assay, DNA interaction studies of platinum(II) complexes, Journal of Biomolecular Structure and Dynamics, (2016) 1-18, doi: 10.1080/07391102.2016.1268071.

XV. S.C. Karad, V.B. Purohit, D.K. Raval, Design, synthesis and characterization of fluoro substituted novel pyrazolylpyrazolines scaffold and their pharmacological screening, European Journal of Medicinal Chemistry, 84 (2014) 51-58, doi: http://dx.doi.org/10.1016/j.ejmech.2014.07.008.

XVI. C.B.I. A. Rattan, Antimicrobials in Laboratory Medicine, (2000) 85–108.

XVII. N.R.F. B.N. Meyer, J.E. Putnam, L.B. Jacobsen, D.E. Nichols, J.L. McLaughlin, , Planta Medica, 45 (1982) 31.

XVIII. K.P. Thakor, M.V. Lunagariya, M.N. Patel, Acetyl pyridine-based palladium(II) compounds as an artificial metallonucleases, Journal of Biomolecular Structure and Dynamics, (2016) 1-13, doi: 10.1080/07391102.2016.1236748.

XIX. M.N. Patel, A.P. Patidar, P.S. Karia, P.A. Vekariya, Cytotoxic, antibacterial and nucleic acid interaction studies of square planar palladium(II) complexes, InorganicaChimica Acta, 419 (2014) 45-54, doi: http://dx.doi.org/10.1016/j.ica.2014.04.037.

XX. J. Marmur, A procedure for the isolation of deoxyribonucleic acid from micro-organisms, Journal of Molecular Biology, 3 2 (1961) 208-IN201, doi: http://dx.doi.org/10.1016/S0022-2836(61)80047-8.

XXI. C.Y. Zhou, Zhao, J., Wu, Y.B., Yin, C.X., Yang,, Synthesis, characterization and studies on DNA binding of a new Cu (II) complex with N1–N8 bis (1-methyl-4-nitropyrole-2-carbonyl) triethylenetetramine., J. Inorg. Biochem., 101 (2007) 10–18.

XXII. C. Icsel, V.T. Yilmaz, Y. Kaya, H. Samli, W.T.A. Harrison, O. Buyukgungor, New palladium(ii) and platinum(ii) 5,5-diethylbarbiturate complexes with 2-phenylpyridine, 2,2[prime or minute]-bipyridine and 2,2[prime or minute]-dipyridylamine: synthesis, structures, DNA binding, molecular docking, cellular uptake, antioxidant activity and cytotoxicity, Dalton Transactions, 44 15 (2015) 6880-6895, doi: 10.1039/C5DT00728C.

XXIII. J.B. Chaires, N. Dattagupta, D.M. Crothers, Studies on interaction of anthracycline antibiotics and deoxyribonucleic acid: equilibrium binding studies on the interaction of daunomycin with deoxyribonucleic acid, Biochemistry, 21 17 (1982) 3933-3940, doi: 10.1021/bi00260a005.

XXIV. F. Leng, W. Priebe, J.B. Chaires, Ultratight DNA Binding of a New Bisintercalating Anthracycline Antibiotic, Biochemistry, 37 7 (1998) 1743-1753, doi: 10.1021/bi9720742.

XXV. C.G. Ricci, P.A. Netz, Docking Studies on DNA-Ligand Interactions: Building and Application of a Protocol To Identify the Binding Mode, Journal of Chemical Information and Modeling, 49 8 (2009) 1925-1935, doi: 10.1021/ci9001537.

XXVI. J.V. Mehta, S.B. Gajera, M.N. Patel, Biological applications of pyrazoline-based half-sandwich ruthenium(III) coordination compounds, Journal of Biomolecular Structure and Dynamics, (2016) 1-9, doi: 10.1080/07391102.2016.1189360.

XXVII. J.R. Lakowicz, Principles of Fluorescence Spectroscopy, Springer, (2006).

XXVIII. L. Zhu, K. Zheng, Y.-T. Li, Z.-Y. Wu, C.-W. Yan, Synthesis and structure elucidation of new μ-oxamido-bridged dicopper(II) complex with in vitro anticancer activity: A combined study from experiment verification and docking calculation on DNA/protein-binding property, Journal of Photochemistry and Photobiology B: Biology, 155 (2016) 86-97, doi: http://dx.doi.org/10.1016/j.jphotobiol.2015.12.015.

XXIX. O. Stern and M. Volmer, Z. Phys.,, 20 (1919) 183.

XXX. R. Frank, H. Rau, Static and dynamic quenching of the emission of excited ruthenium(II) tris(bipyridyl) cation by nickel(II)-tetracyanodithiolene anion, The Journal of Physical Chemistry, 87 25 (1983) 5181-5184, doi: 10.1021/j150643a024.

XXXI. A. Kathiravan, R. Renganathan, Photoinduced interactions between colloidal TiO2 nanoparticles and calf thymus-DNA, Polyhedron, 28 7 (2009) 1374-1378, doi: http://dx.doi.org/10.1016/j.poly.2009.02.040.

XXXII. M. Hong, G. Chang, R. Li, M. Niu, Anti-proliferative activity and DNA/BSA interactions of five mono- or di-organotin(iv) compounds derived from 2-hydroxy-N[prime or minute]-[(2-hydroxy-3-methoxyphenyl)methylidene]-benzohydrazone, New Journal of Chemistry, 40 9 (2016) 7889-7900, doi: 10.1039/C6NJ00525J.

XXXIII. D. Sinha, A.K. Tiwari, S. Singh, G. Shukla, P. Mishra, H. Chandra, A.K. Mishra, Synthesis, characterization and biological activity of Schiff base analogues of indole-3-carboxaldehyde, European Journal of Medicinal Chemistry, 43 1 (2008) 160-165, doi: http://dx.doi.org/10.1016/j.ejmech.2007.03.022.

XXXIV. N.T. Abdel Ghani, A.M. Mansour, Novel Pd(II) and Pt(II) complexes of N,N-donor benzimidazole ligand: Synthesis, spectral, electrochemical, DFT studies and evaluation of biological activity, InorganicaChimica Acta, 373 1 (2011) 249-258, doi: http://dx.doi.org/10.1016/j.ica.2011.04.036.

XXXV. J. Luo, Y. Liu, Q. Chen, D. Shi, Y. Huang, J. Yu, Y. Wang, Z. Zhang, G. Lei, W. Zhu, Synthesis, optoelectronic properties of a dinuclear platinum(ii) complex containing a binary cyclometalated ligand in the single-emissive-layer PLEDs, Dalton Transactions, 42 4 (2013) 1231-1237, doi: 10.1039/C2DT31863F.

XXXVI. A.A. Soliman, O.I. Alajrawy, F.A. Attaby, W. Linert, New binary and ternary platinum(II) formamidine complexes: Synthesis, characterization, structural studies and in-vitro antitumor activity, Journal of Molecular Structure, 1115 (2016) 17-32, doi: http://dx.doi.org/10.1016/j.molstruc.2016.02.073.

XXXVII. D.R. Graham, L.E. Marshall, K.A. Reich, D.S. Sigman, Cleavage of DNA by coordination complexes. Superoxide formation in the oxidation of 1,10-phenanthroline-cuprous complexes by oxygen - relevance to DNA-cleavage reaction, Journal of the American Chemical Society, 102 16 (1980) 5419-5421, doi: 10.1021/ja00536a063.

XXXVIII. P.S. Karia1, P.A. Vekariya1, A.P. Patidar1, •, R.R. Patel2, M.N. Patel, Monitoring the DNA by ruthenium complexes of heterocyclic N,S-donor ligands and evaluation of biological activities, Monatsh Chem, (2015).

XXXIX. J.V. Mehta, S.B. Gajera, P. Thakor, V.R. Thakkar, M.N. Patel, Synthesis of 1,3,5-trisubstituted pyrazoline derivatives and their applications, RSC Advances, 5 104 (2015) 85350-85362, doi: 10.1039/C5RA17185G.

XL. D.L. Boger, B.E. Fink, S.R. Brunette, W.C. Tse, M.P. Hedrick, A Simple, High-Resolution Method for Establishing DNA Binding Affinity and Sequence Selectivity, Journal of the American Chemical Society, 123 25 (2001) 5878-5891, doi: 10.1021/ja010041a.

XLI. H. Soori, A. Rabbani-Chadegani, J. Davoodi, Exploring binding affinity of oxaliplatin and carboplatin, to nucleoprotein structure of chromatin: Spectroscopic study and histone proteins as a target, European Journal of Medicinal Chemistry, 89 (2015) 844-850, doi: http://dx.doi.org/10.1016/j.ejmech.2014.10.063.

XLII. V.T. Yilmaz, C. Icsel, F. Suyunova, M. Aygun, N. Aztopal, E. Ulukaya, Ni(ii)/Cu(ii)/Zn(ii) 5,5-diethylbarbiturate complexes with 1,10-phenanthroline and 2,2[prime or minute]-dipyridylamine: synthesis, structures, DNA/BSA binding, nuclease activity, molecular docking, cellular uptake, cytotoxicity and the mode of cell death, Dalton Transactions, 45 25 (2016) 10466-10479, doi: 10.1039/C6DT01726F.

XLIII. P. Paul, G. Suresh Kumar, Thermodynamics of the DNA binding of phenothiazinium dyes toluidine blue O, azure A and azure B, The Journal of Chemical Thermodynamics, 64 (2013) 50-57, doi: http://dx.doi.org/10.1016/j.jct.2013.04.023.

XLIV. E.C. Long, J.K. Barton, On demonstrating DNA intercalation, Accounts of Chemical Research, 23 9 (1990) 271-273, doi: 10.1021/ar00177a001.

XLV. S.W. Kaldor, B.A. Dressman, M. Hammond, K. Appelt, J.A. Burgess, P.P. Lubbehusen, M.A. Muesing, S.D. Hatch, M.A. Wiskerchen, A.J. Baxter, Isophthalic acid derivatives: amino acid surrogates for the inhibition of HIV-1 protease, Bioorganic & Medicinal Chemistry Letters, 5 7 (1995) 721-726, doi: http://dx.doi.org/10.1016/0960-894X(95)00102-Y.

XLVI. L. Kapicak, E.J. Gabbay, Topography of nucleic acid helixes in solutions. XXXIII. Effect of aromatic cations on the tertiary structures of deoxyribonucleic acid, Journal of the American Chemical Society, 97 2 (1975) 403-408, doi: 10.1021/ja00835a031.

XLVII. R.K. Gupta, G. Sharma, R. Pandey, A. Kumar, B. Koch, P.-Z. Li, Q. Xu, D.S. Pandey, DNA/Protein Binding, Molecular Docking, and in Vitro Anticancer Activity of Some Thioether-Dipyrrinato Complexes, Inorganic Chemistry, 52 24 (2013) 13984-13996, doi: 10.1021/ic401662d.

XLVIII. S. Tabassum, M. Zaki, M. Afzal, F. Arjmand, New modulated design and synthesis of quercetin-CuII/ZnII-Sn2IV scaffold as anticancer agents: in vitro DNA binding profile, DNA cleavage pathway and Topo-I activity, Dalton Transactions, 42 27 (2013) 10029-10041, doi: 10.1039/C3DT50646K.

Received on April 24, 2017.